AD-A099 753 FLORIDA UNIV GAINESVILLE DEPT OF NUCLEAR ENGINEERIN--ETC F/G 20/5
GAIN AND LASING IN NUCLEAR EXCITED EXCIMER LASER SYSTEMS.(U)
APR 81 R A WALTERS, J D COX, R T SCHNEIDER DAS660-79-C-0083

UNCLASSIFIED NL

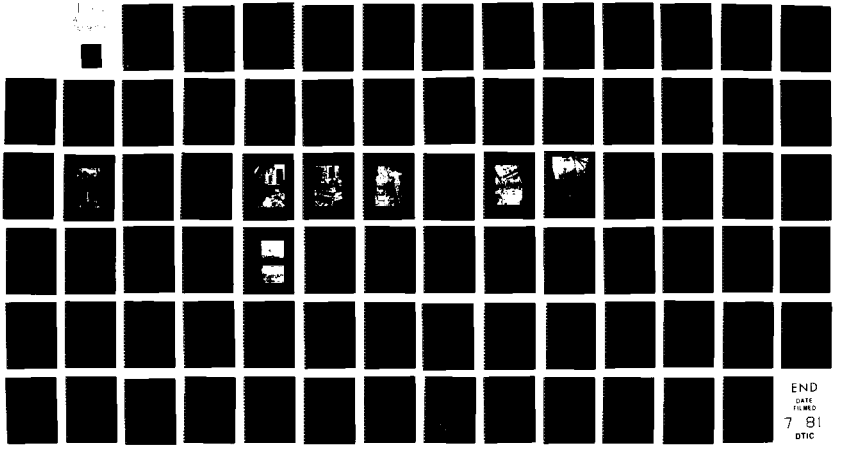

END
DATE FILMED
7 81
DTIC

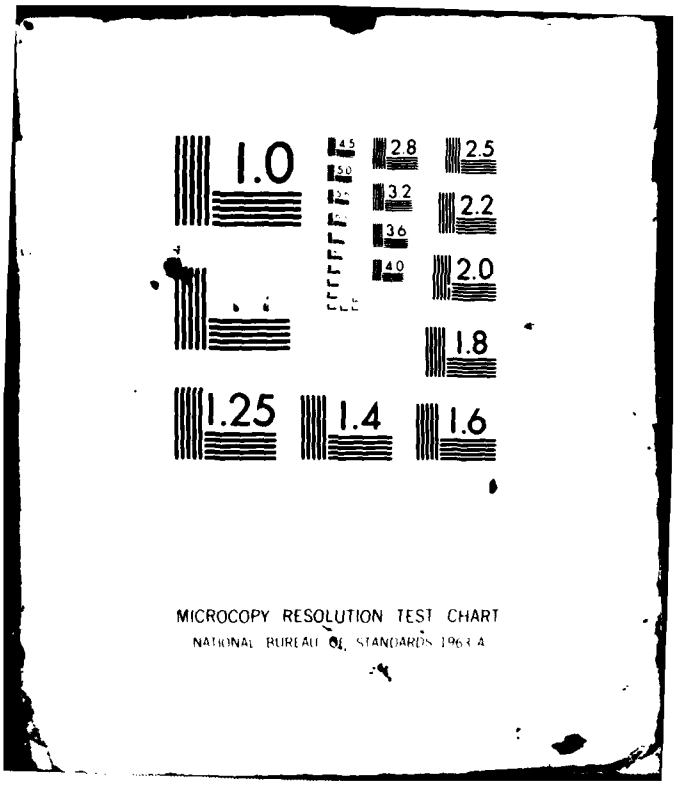
1.0
2.8
2.5
3.2
2.2
3.6
2.0
4.0
1.8
1.25
1.4
1.6
MICROCOPY RESOLUTION TEST CHART
NATIONAL BUREAU OF STANDARDS 1963 A

GAIN AND LASING IN NUCLEAR EXCITED LASER SYSTEMS

DASG 60-79-C-0083

Final Contractor's Report

April 24, 1981

by

Roy A. Walters
John Cox
Richard T. Schneider

Nuclear Engineering Sciences
University of Florida
Gainesville, Florida 32611

Unclassified

SECURITY CLASSIFICATION OF THIS PAGE *(When Data Entered)*

REPORT DOCUMENTATION PAGE

READ INSTRUCTIONS BEFORE COMPLETING FORM

1. REPORT NUMBER

2. GOVT ACCESSION NO. AD-A099753

3. RECIPIENT'S CATALOG NUMBER

4. TITLE *(and Subtitle)*

Gain and Lasing in Nuclear Excited Excimer Laser Systems

5. TYPE OF REPORT & PERIOD COVERED
Final Contractors Report, 29 Jun 79 — 28 Feb 81

6. PERFORMING ORG. REPORT NUMBER

7. AUTHOR(s)

Roy A. Walters
John D. Cox
Richard T. Schneider

8. CONTRACT OR GRANT NUMBER(s)
DASG 60-79-C-0083

9. PERFORMING ORGANIZATION NAME AND ADDRESS

Department of Nuclear Engineering Sciences
University of Florida, Gainesville, FL 32611

10. PROGRAM ELEMENT, PROJECT, TASK AREA & WORK UNIT NUMBERS

11. CONTROLLING OFFICE NAME AND ADDRESS

Ballistic Missile Defense Advanced Technology Center, P.O. Box 1500, Huntsville, AL 35807

12. REPORT DATE
24 Apr 81

13. NUMBER OF PAGES
64

14. MONITORING AGENCY NAME & ADDRESS *(if different from Controlling Office)*

15. SECURITY CLASS. *(of this report)*
Unclassified

15a. DECLASSIFICATION/DOWNGRADING SCHEDULE

16. DISTRIBUTION STATEMENT *(of this Report)*

[illegible] has been approved [illegible] sale; its [illegible] unlimited.

17. DISTRIBUTION STATEMENT *(of the abstract entered in Block 20, if different from Report)*

18. SUPPLEMENTARY NOTES

19. KEY WORDS *(Continue on reverse side if necessary and identify by block number)*

Nuclear pumped lasers, Nuclear flashlamp
Xe_2^* flashlamp, Xenon Difluoride photolysis
XeF(C-A) laser, parasitic amplification

20. ABSTRACT *(Continue on reverse side if necessary and identify by block number)*

A He:Xe nuclear pumped flashlamp laser system based on a burst reactor neutron source has been constructed. The optical output of the flashlamp exceeds 500 joules from 170 nm Xe_2^* fluorescence and 200 joules from Xe and the Xe continuum in the visible. The XeF_2 photolysis XeF (C-A) laser system (483 nm) studied did not lase as expected. Gain (~2% meter) was observed at a lower level than expected. An alternate laser output at 370 nm from S** is suspected. The concept of "parasitic amplification" was

→ Next page

DD FORM 1 JAN 73 1473 EDITION OF 1 NOV 65 IS OBSOLETE
S/N 0102-014-6601

Unclassified
SECURITY CLASSIFICATION OF THIS PAGE *(When Data Entered)*

H02317

developed to explain the discrepancy between calculated gain and lasing and the observed results. Alternate nuclear flashlamp laser concepts and direct nuclear pumped laser systems are reviewed.

GAIN AND LASING IN NUCLEAR EXCITED LASER SYSTEMS

DASG 60-79-C-0083

Final Contractor's Report

April 24, 1981

by

Roy A. Walters
John Cox
Richard T. Schneider

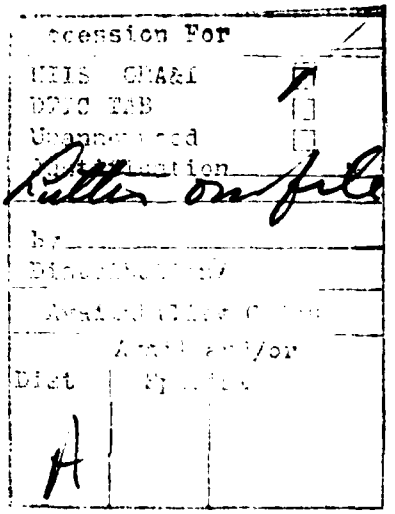

Nuclear Engineering Sciences
University of Florida
Gainesville, Florida 32611

TABLE OF CONTENTS

LIST OF FIGURES

LIST OF TABLES

CHAPTER 1

1.0 INTRODUCTION

Upon completion of the studies of energy transfer from nuclear fission to UV excimer fluorescence (Walters, 1979), it was evident that extremely efficient energy transfer (>50%) was available via the reaction $^{3}He(n,p)^{3}T$ to the production of a Xe_2^* excimer band centered at 172 nm. This efficiency has been verified by several other investigators using electron beams or gamma radiation as energy input (Campbell, 1979; Eckstrom, 1979; Duzy, 1979; Hughes, 1979).

With this vacuum ultraviolet (VUV) flashlamp, one could expect to optically pump a laser with reasonable efficiency. The chosen laser system was photolytic dissociation of XeF_2 to XeF^* (C) with a resultant lasing capability (C-A) in the blue around 480 nm. Since this system is well characterized by ample experimentation using an electron beam pumped Xe_2^* flashlamp (Bischell, 1980) it was estimated to have a high probability of success via nuclear excitation. In this case, a nuclear flashlamp is substituted for the electron beam flashlamp, thus uncoupling the laser kinetics from any nuclear consideration.

Preliminary computer studies by Fisher & Lim (Lim, 1979) at Wayne State University and also by us (See Section 2) showed that even with the relatively long pulse width of a burst reactor (200 microsec.) as compared to the electron beam source (1 microsec.) lasing would still be achieved by increasing the XeF_2 fill gas pressure from the 2 Torr (as used in electron-beam pumped systems) to 7 Torr. This makes use of the high absorption of the 172 nm Xe_2^* band by XeF_2 resulting in production of a time dependent bleaching wave. This inward moving bleaching wave allows for an effective short rise time of the Xe_2^* photon flux in the center of a cylindrical cavity at just the point in time that the thermal neutron flux is reaching a maximum, the optimum point for lasing.

Using our computer codes, we were able to optimize the experimental configuration (Section 3) with respect to the available VUV quartz (suprasil) diameters and the requirements and characteristics of the fast burst reactor facility at the Aberdeen Proving Grounds Pulsed Radiation Facility (APRF).

The experimental procedures concerning lasing, gain, and fluorescence were performed during the weeks of 3 August and 10 August, 1980 and March 2, 1981.

CHAPTER 2

2.0 THEORETICAL CONSIDERATIONS

For research concerning nuclear pumping of lasers, the nuclear reactor and the laser cavity are isolated from each other. The nuclear reactor is used only as a source of neutrons and gamma-rays. A fast burst reactor can provide a 50 microsecond pulse of fast neutrons with a peak flux of 10^{20} nts/cm^2 sec. in close proximity to the surface of the reactor. The neutrons must then be moderated or thermalized to cause nuclear reactions with isotopes of Uranium, Helium, or Boron such as:

$$n + {}^{3}He \rightarrow p + {}^{3}T + 760\ Kev \qquad (2.1)$$

$$n + {}^{10}B \rightarrow + {}^{7}Li + 4.8\ MeV \qquad (2.2)$$

$$n + {}^{235}U \rightarrow ff + ff + n + 180\ MeV \qquad (2.3)$$

One of the outstanding features of nuclear pumping is that there are no barrier problems to overcome as with e-beam or proton-beam pumping. Neutrons can easily penetrate the laser cavity containment. The high energy charged particles produced by nuclear reactions can then internally excite the lasing medium creating a population inversion. If the nuclear reaction source material is in a gaseous state such as ^{3}He or UF_6, a homogeneous mixture of fuel and lasant gases can be made thus creating a fissioning plasma. High energy reaction particles from uranium and Boron foils have also been used to create nuclear induced plasmas. NPLs have been developed using both volume and wall nuclear reaction sources. The most advantageous volumetric nuclear excitation source is UF_6. If enriched UF_6 could be used as a pump source, a self-critical NPL could be envisioned thus combining the laser and the reactor. Unfortunately, UF_6 has a high optical absorption cross section and has shown a propensity to quench excited states. (Walters, 1979)

The highest power density achievable from these systems is on the order of 50 Kw/cm^3. In comparison to e-beam and discharge pumped systems that have power densities on the order of 1 Mw/cm^3, nuclear pumping is a low power system. However, the excitation volume and the pump pulse duration for NPLs can be quite large, thus producing a high output energy device.

The most promising feature of Nuclear Pumped Lasers (NPL) is their inherent scalability to high energy. In order to achieve this, an efficient energy transfer between the pump source and the lasing transition must be maintained. Nuclear Pumped Laser systems, in the past, have been designed such that the nuclear interactions yielding high energy charged particles have taken place within the laser cavity. Although oscillation has been achieved in some cases, it has become evident that direct nuclear excitation has detrimental effects that must be mitigated. (Jalufka, 1979) These effects include direct population of the lower laser state by nuclear excitation and gas heating or by quenching of the upper laser state by UF_6 and other species. Most NPLs demonstrated to date are recombination lasers. Depending on the gas, the inversion is created by dissociative recombination or 3-body recombination. So far there are only a few cases (CO, He-Ne, CO_2) where this is not the case.

To improve the performance of NPLs, the nuclear excitation must be uncoupled from the laser kinetics and still provide for efficient energy transfer to the upper laser level. This concept has given rise to a new type of NPL designed to obtain this goal. (Rowe, 1980).

The search for a high energy visible laser candidate has centered on the excimer molecules.

The term "excimer", itself a contraction of the phrase "excited Dimer," refers to the molecule formed by association of one excited atom

(or molecule) with a ground state atom (or molecule). Originally the usage was restricted to a bound complex of identical atoms (e.g., Xe_2^*) in which the interaction between the ground state atoms was purely repulsive. Since the ground state of these species is unstable, this system provides a natural laser inversion with energy extraction determined by the laser cavity design, the stimulated emission cross section and the upper state lifetime.

The main obstacle to overcome in scaling the excimer laser to high powers (>1 MW) is a mechanism for depositing large amounts of primary excitation energy into the gas in the laser cavity in a short period of time. Excimer lasers have been pumped by relativistic electron-beams and high voltage electric discharges. (Brau, 1979) At the present time the best efficiency reported with electron-beam pumping is comparable to that achieved with discharges (on the order of 1% overall). The largest pulse energy achieved with an electron-beam (about 350 J) is almost an order of magnitude greater than the best result reported from a discharge (about 50J) (Brau, 1979)

Excimer lasers are by nature short-wavelength lasers, many lasing in the VUV or XUV. (Hutchinson, 1980) There are particular problems associated with these types of lasers. First, lets consider the pumping power density required to produce a reasonable gain coefficient per unit length. The stimulated emission cross section is given by:

$$\sigma = \lambda^4(8\pi\tau\Delta\lambda_c) \tag{2.4}$$

where λ is the transition wavelength and τ is the spontaneous lifetime. The pumping power per unit length is, therefore, given by:

$$P = (8\pi hc^2\Delta\lambda)/(\lambda^5\eta\phi) \tag{2.5}$$

where ϕ is the quantum efficiency and η is the efficiency of population of the upper laser level. The difficulty of pumping short-wavelength

lasers is indicated by this λ^{-5} scaling law. Typical pumping power densities required to produce gain coefficients of 0.1 cm^{-1} (which are typical of laser oscillators) for excimer lasers are on the order of $10^7 - 10^6$ watts/ cm^3.

There are few, if any, energy sources that can maintain this high pumping power requirement for continuous wave operation. It can be shown that the Dimers (e.g., Xe_2^*, Kr_2^*, Ar_2^*) can be lased in the continuous wave mode if the gas is cooled to avoid thermal population of the lower laser level by atomic collision. This is possible because nothing is consumed in the excitation process. In the case of the rare gas halides, the halide donor is consumed in the excitation process that provides atomic halides (e.g., F, F^*, or F-) for the formation of the excimers. Depletion problems are mitigated by the use of a short rise-time pump pulse. A short pulse is defined here as a pumping pulse with a FWHM on the order of the upper state lifetime. In the case of excimers, this is less than 100 nanoseconds. For pump pulses that are much longer than this (>0.5 microsec.) the excimer lasers operate in a quasi continuous wave mode. Laser action will terminate with the depletion of the halide donor or the buildup of quenching agents.

In order to achieve nuclear pumping of excimers, the rise time of the thermal neutron pulse must be drastically decreased over that available from a burst reactor (80 μs). In a photolytic system the rise time of the pump pulse can be artificially increased by the use of an optically thick, slow diffusion, depletable (to the photon pump pulse) laser medium. The slow leading edge of the photon pulse is absorbed in the outer region of a cylindrical cavity creating a bleaching wave as the absorber is burned out. If this bleaching wave reaches the center of the cavity at the point in time that the pump pulse is peaking, a very fast rising pulse is created at the center of the cavity. Although

direct nuclear pumping of $XeF^*(B)$ has been demonstrated at the UFTR at the University of Florida (Walters, 1979), at the TRIGA reactor at the University of Illinois (Miley, 1978) and at the Fast Burst Reactor at the Aberdeen Proving Grounds (DeYoung, 1979), no lasing action has been achieved with these homogeneous systems. Nuclear induced photolytic pumping of XeF^* may achieve lasing with a high-Q cavity.

The use of a photon source to pump rare gas halide lasers, such as in the photolysis of XeF_2 by Xe_2^* excimer emission to the C state of XeF^*, and subsequent lasing in the blue, allows the uncoupling of laser kinetics from the process of excitation. This, in fact, has been demonstrated by the Photolytically Pumped XeF(C-A) Blue-Green Laser developed by the Molecular Physics Laboratory at the Stanford Research Institute. They have achieved a 5 Joule output pulse centered at 483 nanometers from the XeF(C-A) lasing transition. (Bischel, 1979) In this case the 5 atmosphere Xenon flashlamp was used to absorb the 600 KeV electron-beam and fluoresced at 172 nanometers transfering energy to the laser cavity. Direct electron-beam excitation is not desirable here because of the low stopping power of the lasing buffer gas (1.5 atm. N_2).

Upon the completion of studies of energy transfer from nuclear fission to UV excimer fluorescence, it was evident that extremely efficient energy transfer (>50%) was available via the reaction $^3He(n,p)^3T$ to the production of a Xe_2^* transition at 172 nanometers. (Walters, 1979) With this vacuum ultraviolet (VUV) lamp, one could, with reasonable efficiency, optically pump a laser. The chosen system was photolytic dissociation of XeF_2 to XeF^* (C) with resultant lasing capability (C-A) in the blue around 480 nanometers. Since this system is well characterized by ample experimentation using an electron-beam pumped Xe_2^* flashlamp, it was estimated to have a high probability of success via nuclear excitation.

This is because a nuclear flashlamp has been substituted for the electron-beam pumped flashlamp, thus uncoupling the laser from any nuclear consideration.

Preliminary computer model studies done at the University of Florida (Walters, June, 1979) and by Ed Fisher at Wayne State University (Fisher, 1979) both show that even employing the pulse width (200 microseconds) of a burst reactor which is long compared to the electron-beam source (1 microsecond) lasing could still be achieved if the XeF_2 fill gas pressure is increased from 2 Torr (e-beam) to 7 Torr. This makes use of the high absorption of XeF_2 of the 172 nanometer band to produce a time dependent bleaching wave. This inward moving bleaching wave allows for an effective short rise time of the Xe_2^* pumping pulse in the center of a cylindrical cavity at just the point in time that a burst reactor derived thermal flux is reaching a maximum, the optimum point for lasing.

Utilizing these computer models it was possible to optimize the experimental configuration with respect to the available VUV quartz (suprasil) diameters and the requirements and characteristics of the fast burst reactor facility at the Aberdeen Proving Grounds Pulsed Radiation Facility. This is discussed in the following chapter.

2.1 MODELING

XeF Kinetics

The structure of the XeF^* molecule is atypical. As shown in Figure 2.1 the X or ground state manifold is bound so that transitions from B-X (350 nm laser transition) are bound-bound. Most excimer systems are bound-free. Fortunately, the X manifold is thermally unstable and easily dissociated. Another unusual characteristic of XeF^* is the location of the C state manifold. It is located with the same Bohr radius at approximately 0.075 eV below the B state. In excimers, the C state is normally located above the B state. The transitions from the C states, C-A, are

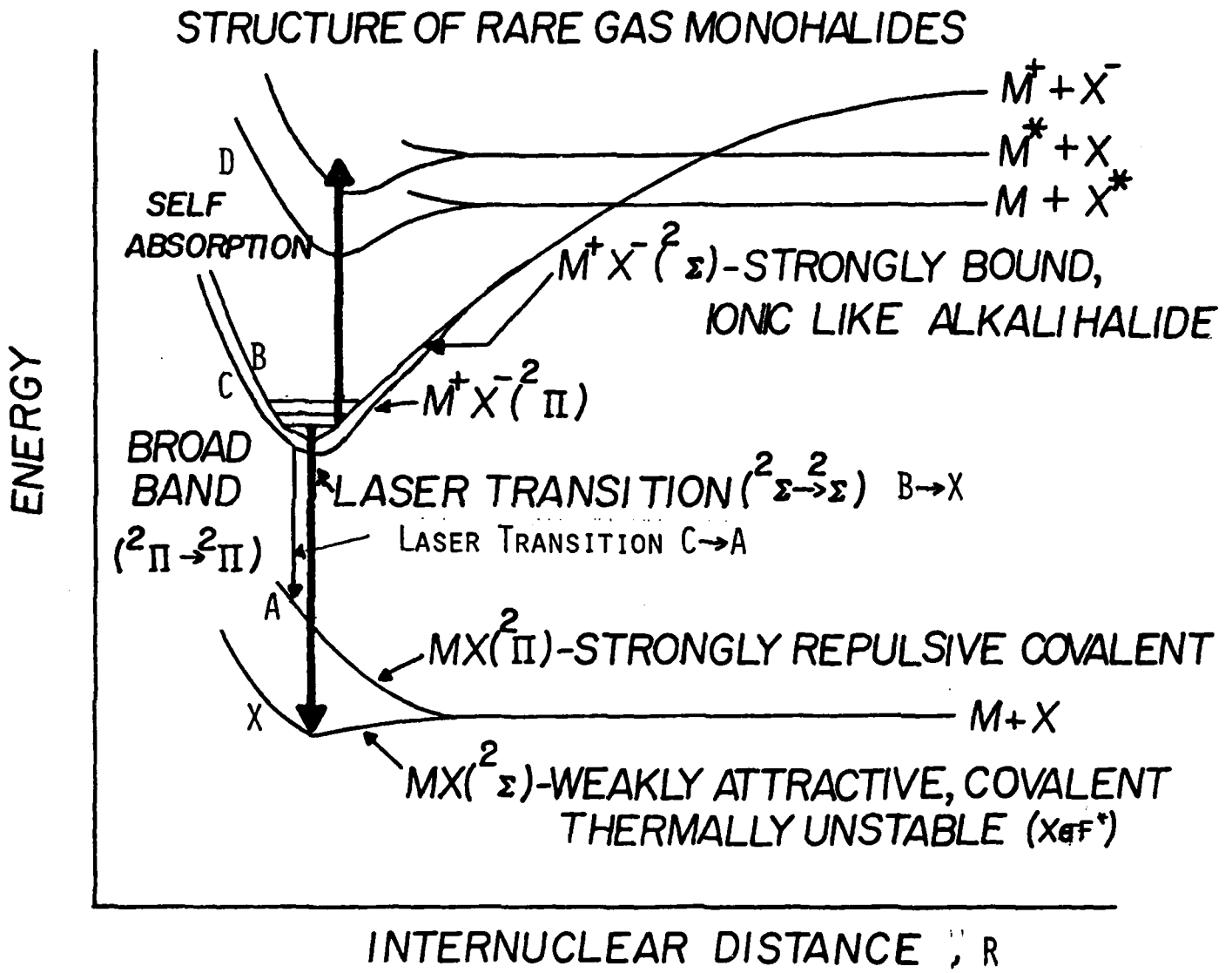

FIGURE 2-1. XeF* ENERGY LEVELS

bound-free and thus represent a non-bottleneck laser system. C-A transitions generate the broad-band emission shown in Figure 2.2 centered around 483 nanometers. Lasing on C-A has been shown for photolytic, electron-beam and electron discharge pumping. Coupling between the B and C states will favor the C state if external influences are alleviated. That is, thermal electrons, high gas temperatures or photoelectrons are not present. Since the B and C states have quantum numbers which differ by one unit, the rotational term of the molecular Hamiltonian is responsible for mutual interaction of these states. Thus, it is possible that B-C intersystem crossing occurs even without collisions. Whatever the actual coupling (still under investigation), spontaneous emission ratios of up to 20, C-A/B-X have been observed under ideal conditions (e.g., photolytic pumping of XeF_2 in a diluent of N_2 and SF_6). As the temperature increases, this ratio decreases. (Kline, 1979) Since the spontaneous emission lifetime of the B-X transition is ~19 nanoseconds and that of the C-A transition is ~115 nanoseconds, the transfer to the C state must be dominant.

The purpose of SF_6 on the gas mixture is to reduce the population of thermal electrons or photo-electrons to a negligible level. This reduces both electron quenching reactions and any effects of thermal electrons on the kinetics of the B-C relaxation.

XeF^* (C) Kinetics

The dominant quenching reaction of the C state is collision with XeF_2 or its products, Xe and F_2. There is a question about the role of F_2 in the system and whether or not it recombines with Xe^+ or Xe^* to form XeF^* or attaches to SF_6 to produce SF_7. In this study, the recombination of F into F_2 was assumed to be the worst case. As stated above, the greatest population of XeF^* (C) can be obtained via a short

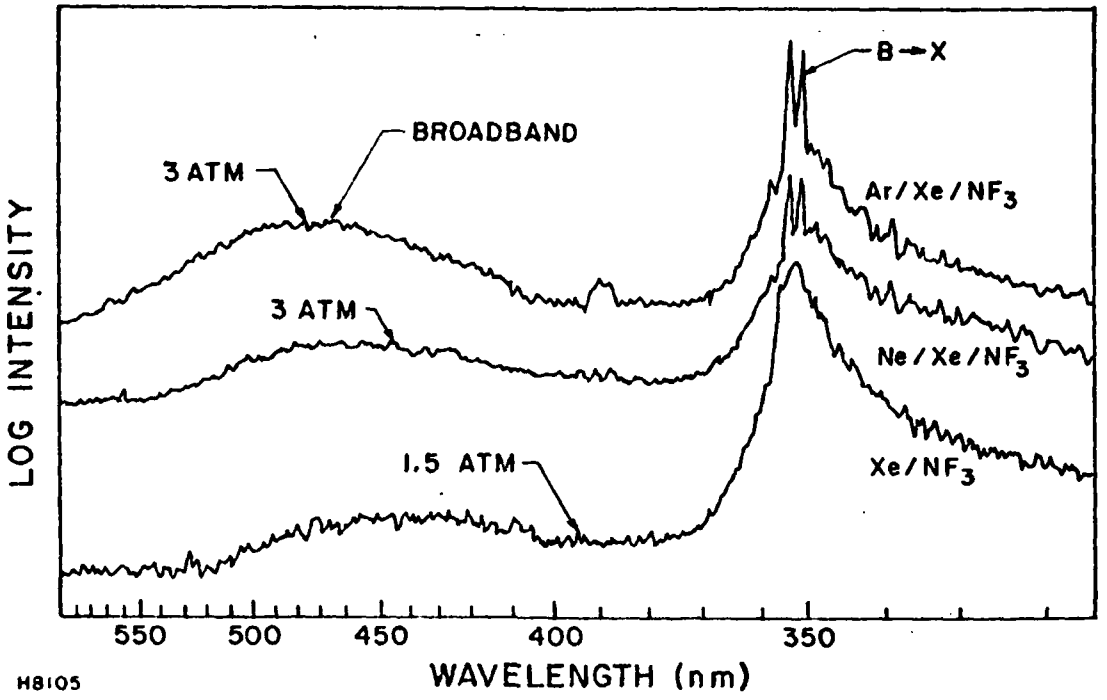

FIGURE 2.2. SPECTRA FOR B → X AND BROADBAND EMISSION C-A FOR VARIOUS INERT GAS/NF_3 MIXTURES.

pulse injection of Xe_2^* radiation. This pulse would burn out the XeF_2 and produce only XeF^* plus a small concentration of F_2. No Xe or XeF_2 quenching would be present. This, of course, may not be practical so a combination of excitation and quenching plus some spontaneous emission produce the population of XeF^* (C). Another important factor to consider in the generation of XeF^*(C) is the optical "thickness" of XeF_2 to 172 nanometer Xe_2^* photons. In a coaxial Xe flashlamp XeF_2 system, 172 nanometer excimer photons must burn their way to the center of the inner cylinder creating a bleaching wave or avalanche of photons. This, typical of electron-beam pumped systems, results in local increase in the XeF^* (C) population due to the instantaneous decrease in the local population of XeF_2. The only other loss in the system is the removal of XeF^* (C) by stimulated emission before quenching reactions can take place.

System Model

Rate constants for the photolytic system have become available allowing the assembly of a kinetic system model. The set of nonlinear differential equations shown below represents the time dependent population of XeF^* (C).

C state population

$$\frac{dN_1}{dt} = \alpha_1 N_2 - K_{12} N_1 N_2 - \alpha_2 N_1 - K_{13} N_3 N_1 - K_{14} N_4 N_1 - \lambda N_1$$

XeF_2 destruction

$$\frac{dN_2}{dt} = -\alpha_1 N_2$$

F_2 formation

$$\frac{dN_3}{dt} = \frac{1}{2} (\alpha_1 N_2 + \lambda N_1 + K_{12} N_1 N_2 + K_{13} N_3 N_1 + K_{14} N_4 N_1 + \alpha_2 N_1)$$

Xe formation

$$\frac{dN_4}{dt} = \lambda N_1 + K_{12}N_1N_2 + K_{13}N_3N_1 + K_{14}N_4N_1 + \alpha_2 N_1$$

where

N_1 = $XeF^*(C)$ population

N_2 = XeF_2 population

N_3 = F_2 population

N_4 = Xe population

α_1 = $\phi_{1720}(t)\ \sigma_{XeF_2}$; VUV photon flux x dissociation cross section

$$\sigma XeF_2 = \begin{cases} (8.5 \times 10^{-18} cm^2,\ L^3) \\ (6 \times 10^{-17} cm^2,\ SRI) \\ (3.62 \times 10^{-17} cm^2,\ avg) \end{cases}$$

α_2 = $K_{SF6}\ N_{SF6}$; $K_{SF6} = 3 \times 10^{-14} cm^3/sec$

λ = $0.693/\tau_{nc}$; τ_{nc} = 115 ns

K_{12} = $K_{XeF_2}(C)$, (quench) = $1.8 \times 10^{-10}\ cm^3/sec$

K_{13} = $K_{F_2}(C)$ = $1 \times 10^{-10}\ cm^3/sec$

K_{14} = $K_{Xe}(C)$ = $2 \times 10^{-11}\ cm^3/sec.$

This elementary model does not include several terms which will be needed in the future to improve accuracy. The first of these is the kinetics term for B-C state mixing. This is still not well defined and depending on the mechanisms involved, the elimination of this term, as has been done in the above set of equations, will produce an error estimated to be 10%. The additional term of stimulated emission $\phi\sigma_{SE}N_1$ is added where appropriate in order to assess the capability of removing power from such a system. It will also provide an estimation of saturated gain.

Solutions to the equation set are not trivial but certain uncoupled approximations can be made because of the relatively slow change in

input power (172 nm) vs. the gas kinetic reaction times. These include a term for the Xe and F_2 population where over the sample interval, i,

$$N_{4_i} = \sum_{i}^{i} (\alpha_{1_i} N_{2_i} \Delta t) - N_{1_{i-1}}$$

Thus the values of the Xe (N_4) population are based upon the total number of XeF_2 (N_2) molecules destroyed and the population of XeF^* (C) (N_i) from the previous interval.

Solutions to N_1 (XeF^* (C)) are obtained by inserting a time dependent function for the 172 nm flux and integrating (finite difference method) through the equation set with a fixed step size (Δt).

The energy input (thermal flux) was modeled by the following function:

$$\phi(t) = \phi_0 \operatorname{sech}^2[(4.0 \times 10^4) t-2]$$

where $\phi_o = 1 \times 10^{17}$.

An exponential function was used from t = 0 to 25 microsec. This provides a thermal neutron pulse and subsequently a photon pulse of approximately 200 microseconds FWHM peaking at 1×10^{17} nts/cm^2sec.

Figure 2.3 shows the pump pulse and the corresponding XeF(C) fluorescence pulse. The maximum XeF (C) state density was predicted to be $1.22 \times 10^{13} cm^{-3}$. This was derived using a slab geometry with no geometrical focussing or bleaching wave that would occur in cylindrical geometry. Using this elementary computer model, a parametric study of initial conditions produced the approximate partial pressures of the lasant gases required to obtain the maximum output power of the laser cavity. The cavity design (described in the next chapter) was obtained from an intera-iterative procedure using data obtained from the code and the practical limitations of the available hardware.

An extensive computer code generated by Fisher & Lin at Wayne State University was used to predict the optimum lasant gas pressures and cavity

Thermal Flux

peak - 1. x 10^{17} n/cm^2-sec

at - 110 microseconds

XeF (C) cm^{-3}

peak - 1.22 x 10^{13}

at - 55 microseconds

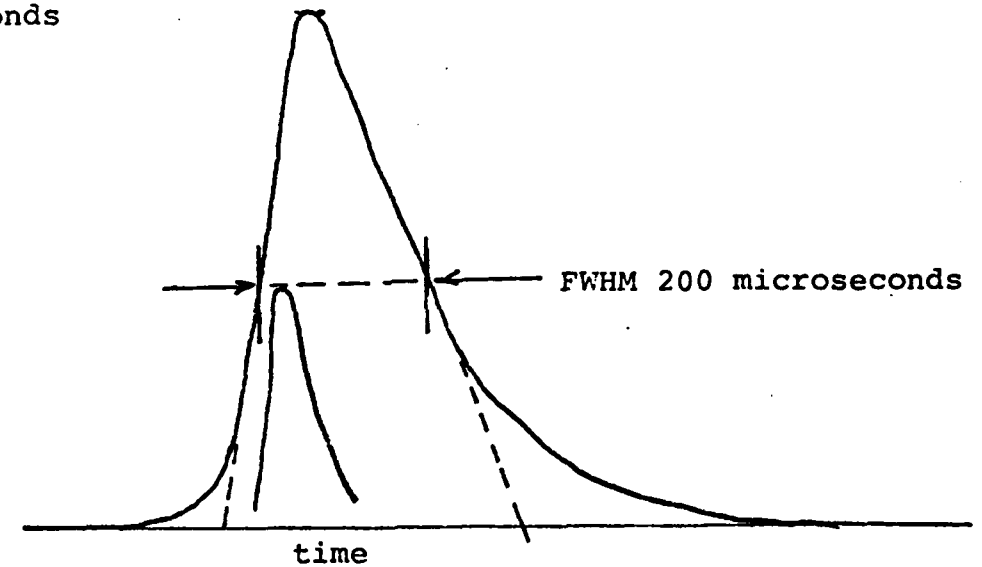

FIGURE 2.3. THERMAL FLUX PROFILE AND FLUORESCENCE PROFILE

Q to produce the maximum output for the experimental conditions and practical limitations mentioned above. A maximum XeF(C) state density predicted by the improved code was 2.4 x $10^{13}cm^{-3}$ based on the cylindrical geometry and extensive energy deposition and gas kinetics considerations. This corresponds to an initial gas fill pressure of $XeF_2:N_2:SF_6$ (7:1000:20 Torr) and a 200 cm 94% cavity (at 480 nm).

The remaining discussion in this chapter evolved from the work done by Fisher and Lim (Lim, 1981).

In order to achieve a lasing action, the number density of upper laser level has to overcome the threshold value of the system. Small signal gain, $N\sigma$, where N is an upper laser level population (cm^{-3}) and σ is a stimulated emission cross section (cm^2), has to be greater than the total loss of laser photons. The threshold number density can be calculated by the following

$$N = \frac{1}{\sigma} \left(\frac{LN(R_1 \cdot R_2 \cdot R_3 \cdot R_4 \cdot R_5)}{(2L)} + \gamma_i \right)$$

Where R_1 through R_5 are the cavity mirror reflectivities, σ is a stimulated emission cross section, and γ_i is an intrinsic loss. For the experimental configuration, the calculated XeF(C) lasing threshold number density calculated by Wayne State bleacher code is 6 x $10^{12}/ cm^3$ with $R_1 \cdot R_5$ = 0.98, L = 280 cm, and γ_i = 6.0 x $10^{18}/cm^2$ without including any intrinsic cavity losses. With the addition of a 10^{-4}/cm intrinsic cavity loss, the lasing threshold number density of XeF(C) becomes 2.3 x $10^{13}/cm^3$, (the experimental conditions).

Thus, in order to predict the absolute laser power correctly, a knowledge of the total intrinsic cavity losses is necessary. Threshold will not be reached for the experimental conditions if the intrinsic loss is greater than about 2.0 x 10^{-4}cm, because a XeF^*(C) number density of (2.0 x $10^{-4}cm^{-1}$/5.0 x 10^{-18} cm^2 = 3.3 x $10^{13}/cm^3$) is required in order to overcome only this intrinsic loss.

The laser output power will be substantially reduced from an order of 20 Kw with a 10^{-5}/cm intrinsic loss to a mere 0.7 watt with a 10^{-4}/cm intrinsic loss. This suggests that the laser cavity is extremely sensitive to impurities and other loss mechanisms. In the development of the complex Wayne State computer code, the cross sections and rate coefficients that were obtained from empirical data had large uncertainties. This imposes some uncertainty in the predicted values of the upper laser level population density and other critical values. Although these uncertainties can be estimated, the correct values must be obtained for more reliable analysis.

Noting the results of these calculations, the uncertainties involved in their generation, and the low power condition imposed by the moderated neutron flux, it is evident that the laser will operate on a marginal basis. Overall gain measurements are expected to yield values on the order of a few percent per meter, while as stated above the laser output power can be expected to be anywhere from a few kilowatts to a few milliwatts depending on the actual cavity losses.

CHAPTER 3

3.0 LASER EXPERIMENT DESIGN AND BURST REACTOR INTERFACE

The design and construction of XeF_2 laser system was undertaken with the understanding that neither the reactor nor the laser system to be constructed could be ideal. Trade studies associated with the computer analysis of Chapter 2 provided insight into the compromises that were made. For example, one must concentrate the thermal neutron flux at the location where Xe_2^* is to be generated but it is also necessary to maximize the length of the active region of the cavity. These are conflicting requirements since an increased length implies further distance from the reactor and thus lower neutron flux.

Figure 3.1 displays the final design of the laser system which is the optimal configuration for the constraints imposed by the reactor system.

The laser/gain cell was designed to be completely modular so that maximum flexibility is available. Module fittings are all standard 2-1/2" Varian vacuum flanges. As shown in Figure 3.1, the laser system surrounds the reactor. It consists of four coaxial flashlamps containing 3.2 amagat of ^3He and 1 amagat of Xe. The inner walls of the four flashlamps are made of suprasil in order to allow the VUV energy to penetrate into the center region which is filled with a partial pressure of XeF_2 of 7 Torr and approximately 1.5 atmospheres of N_2. An SF_6 partial pressure of 15 Torr was also added for removal of free thermal electrons. Other gas fills were also used.

The containment wall of stainless steel is surrounded by a high density polyethelyne moderator and a B^{10} blanket flux trap which allows fast neutrons to enter and thermalize but does not allow thermal neutrons

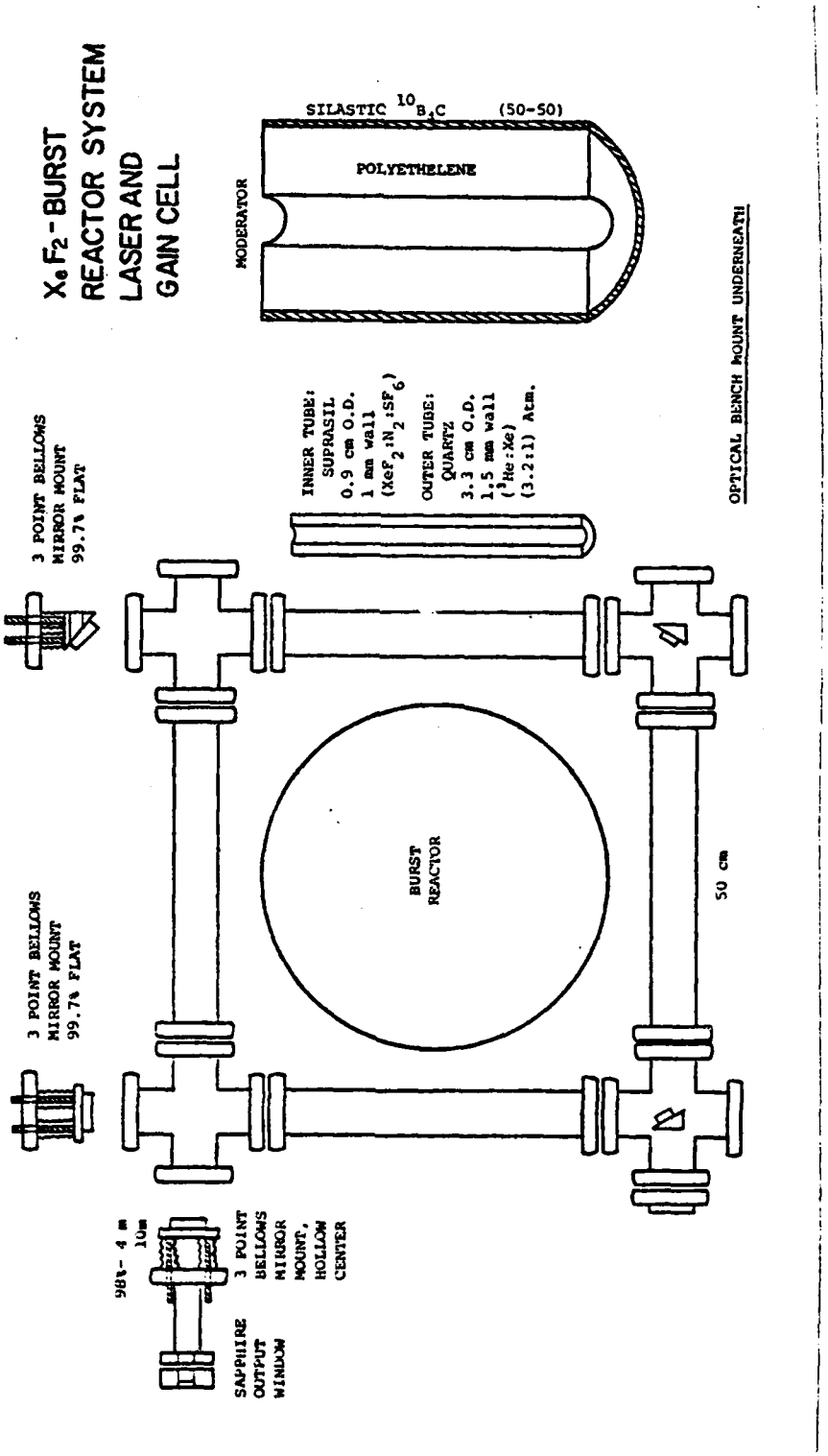

FIGURE 3.1. LASER/GAIN CELL SCHEMATIC

to exit and interfere with reactor operation. On three corners of the ring, beam steering mirrors (99.7% reflective) are placed. In the fourth corner both the output and the 99.7% return mirror are placed at 90°, generating a folded optical cavity of stable hemispherical design. Figure 3.2 shows the actual device as mounted on a stable I-beam platform. The reactor is positioned in the center of the laser and the return and output mirror structures are on the left. All mirrors were purchased as fluorine resistant and 99.7% reflective at 45° and 90° incidence (except the output spherical mirrors at 98%).

3.1 TRADE STUDIES

In the trade studies, the task was to optimize both the density of XeF^* (C) at the center of the coaxial tube and the Q of the cavity at 480 nm.

The good mechanism to achieve maximum upper state population at the tube center is a bleaching wave. Thus, a careful calculation of incoming Xe_2^* band emission was required along with an optimization of the diameter of the excitation region. Although many materials were considered for the flashlamp wall only suprasil was available in the required diameters and lengths. A more preferable laser system design consisting of a folded path in a slab geometry was not implemented due to the unavailability of suitable materials. The largest suprasil disk diameter available was 2". A design based on this would not provide (even in groups) a suitable excitation length within the constraints of the reactor system. Since XeF_2 has 4 Torr partial pressure at 30°C that exponentially rises at higher temperatures, operation much above 30°C was not possible. This would require precise heating of the total system which was not practical under the given circumstances. A smaller diameter tube provides greater optical advantage due to the concentration of the flashlamp light but complicates alignment and requires a higher XeF_2 partial pressure for

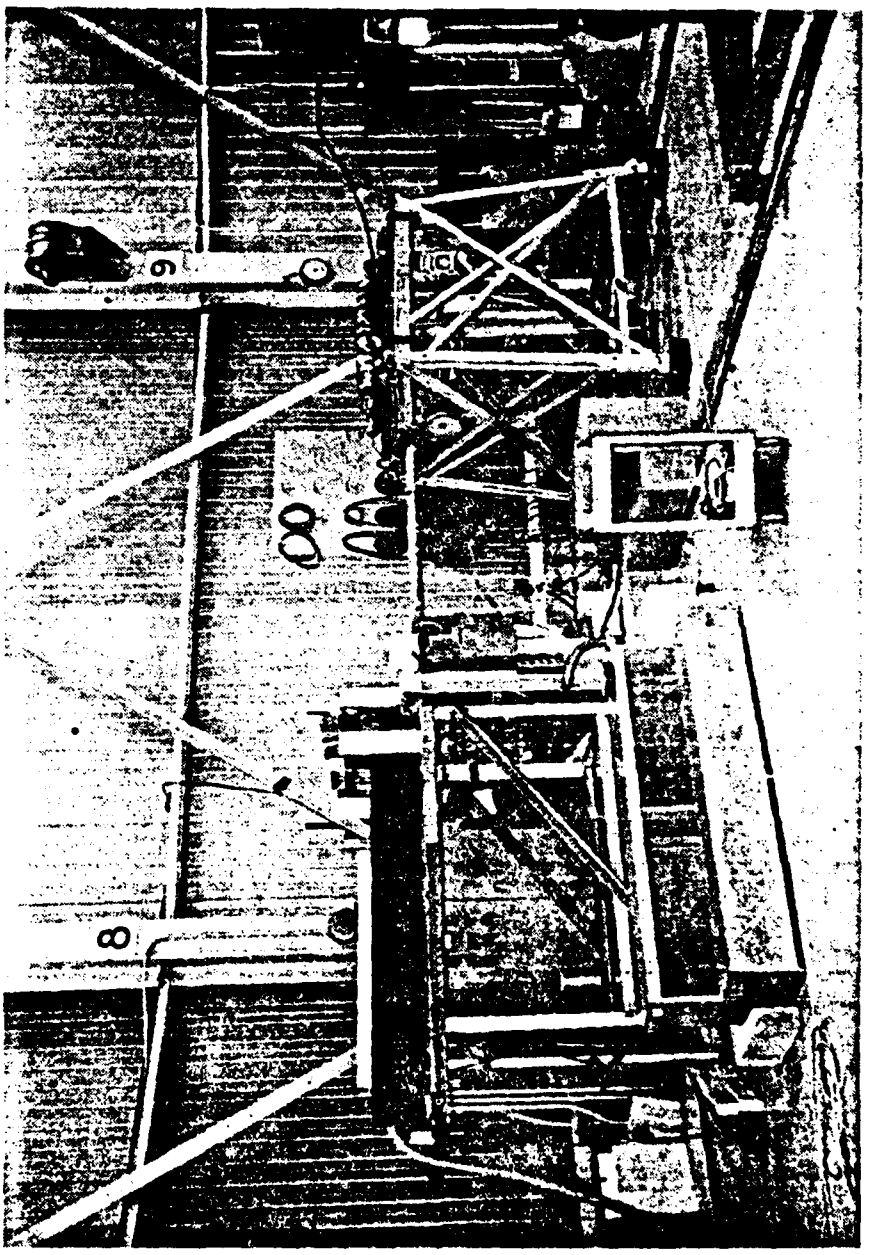

FIGURE 3.2. EXPERIMENTAL SET-UP

establishment of the bleaching wave. A tube ID of 0.7 cm was chosen as an appropriate compromise. This selection is based on the maximum achievable ^{3}He partial pressure in the flashlamp at LN_2 temperatures required by the fill technique (to be reviewed later) and the suitability of the resultant 7 Torr XeF_2 required partial pressure to optimize the bleaching wave.

Fast neutrons exit from the reactor at a peak rate of about 10^{20} n/cm^2sec in a 50 μs pulse of about 30 μs rise time. Since the absorption cross section of ^{3}He is negligible for fast neutrons and is 5327 barns for thermal neutrons, a moderator is required. High density polyethelene was used. A 7.5 cm moderator wall was chosen because thermal flux data using this size was available from earlier NPL experiments (NASA). A ^{10}B blanket around the moderator acts as a flux trap.

The thermal neutrons arrive at the edge of the ^{3}He filled tube where the heavily absorbing ^{3}He causes a flux depression. The trades, in this case, resulted in adjusting the pressure of ^{3}He to the maximum achievable (dictated by the fill technique used) and the flashlamp section diameter to a minimum in order to generate the highest ^{3}He reaction rate possible at the suprasil surface where the photon concentration needs to be the greatest. The flux depression was 70% at the inner wall with a total flux utilization of 30% in the ^{3}He using a 3.3 cm OD quartz outer tube.

A system using standard 2-1/2" Varian components was used to contain the flashlamps.

Safety considerations for tritium generation required triple containment (see Appendix 1, Safety Analysis), 1) a sealed coaxial flashlamp, 2) the outer stainless steel containment, and 3) a tritium absorption system at the pump station outlet (which then exited through the reactor

ventilation system). Since lasing was estimated to occur with a 200 cm cavity of Q = .92, brewster angle corner sections and output sections were not considered. Only internal mirror design would be possible.

XeF_2 is very corrosive to all "workable" vacuum materials except stainless steel and a few nickel alloys. Thus, all moving internal parts must be constructed of stainless steel. The mirror mount system for all corners and end positions was constructed without organic seals that require silicon grease. Figure 3.3 shows examples of the bellows supported design based on standard vacuum mounts. All systems were pressure tested and found adequate. The coaxial flashlamps were tested to destruction at 7 atm, far above the expected load. 99.7% reflective end and corner mirrors (480 nm) were purchased with coatings certified fluorine proof. The output mirror was 98% at 480 nm. The cavity Q was 0.968, .048 above that estimated to be required for lasing.

Figure 3.4 shows the laser cavity with the Aberdeen Proving Grounds reactor in place; Figure 3.5 the reactor and support crane.

The ^{3}He:Xe flashlamps were by requirement of space and safety, sealed without the use of valves. The flashlamps were filled and sealed by the following procedures:

1. quartz tubes were connected to a gas manifold and evacuated.
2. One atmosphere of Xe was added and the tubes were valved off from the manifold.
3. The tubes were then immersed in liquid nitrogen (LN_2), freezing out the Xe.
4. High pressure ^{3}He was added to the super cooled tubes until a -200°C pressure of 700 Torr was reached. Then the tubes were once again valved off from the manifold.
5. While the tubes were continuously cooled by the liquid nitrogen, the quartz fill tube was pinched off with an oxy-acetylene torch.

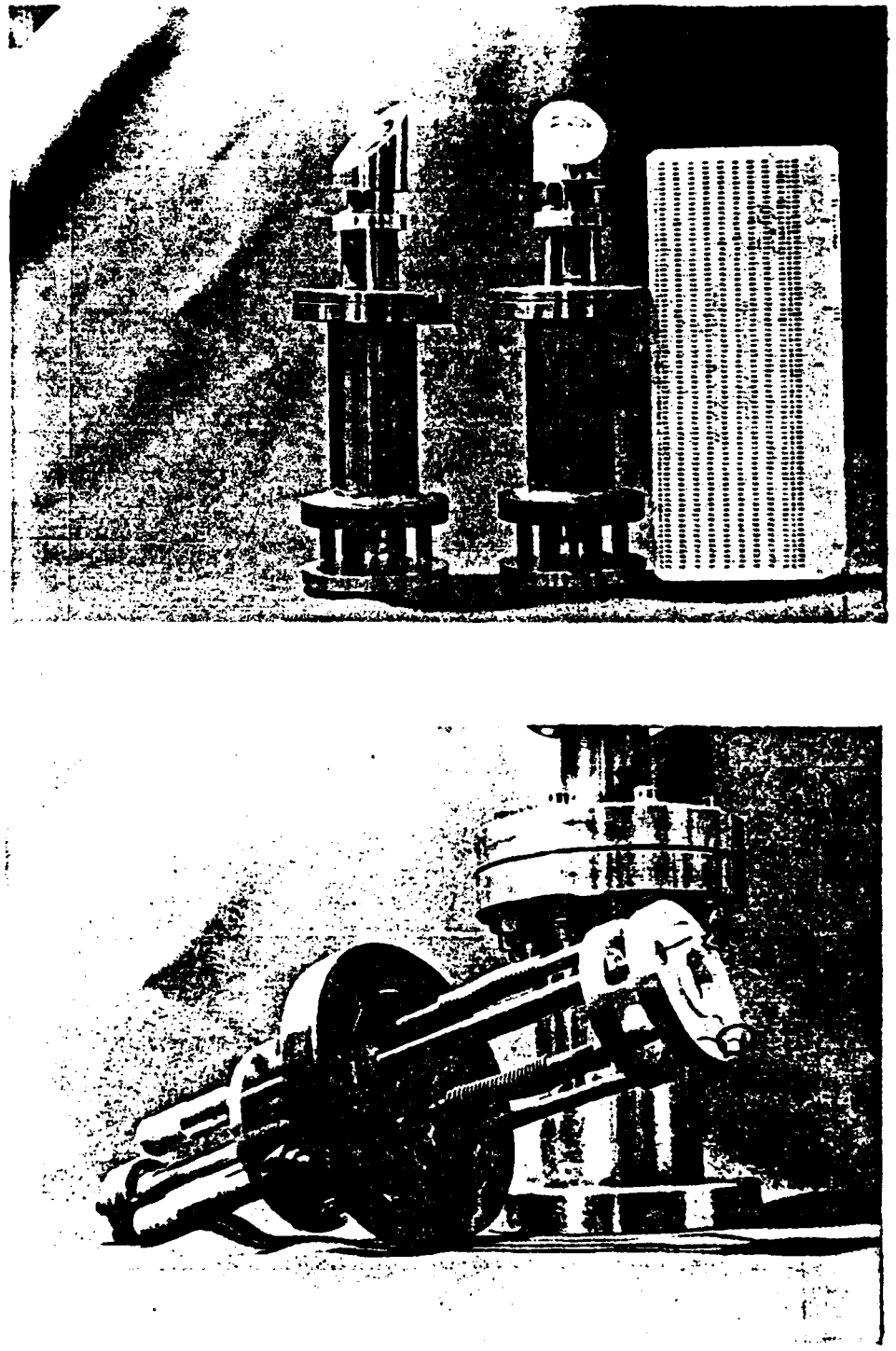

FIGURE 3.3. VACUUM FEEDTHROUGH MIRROR MOUNTS

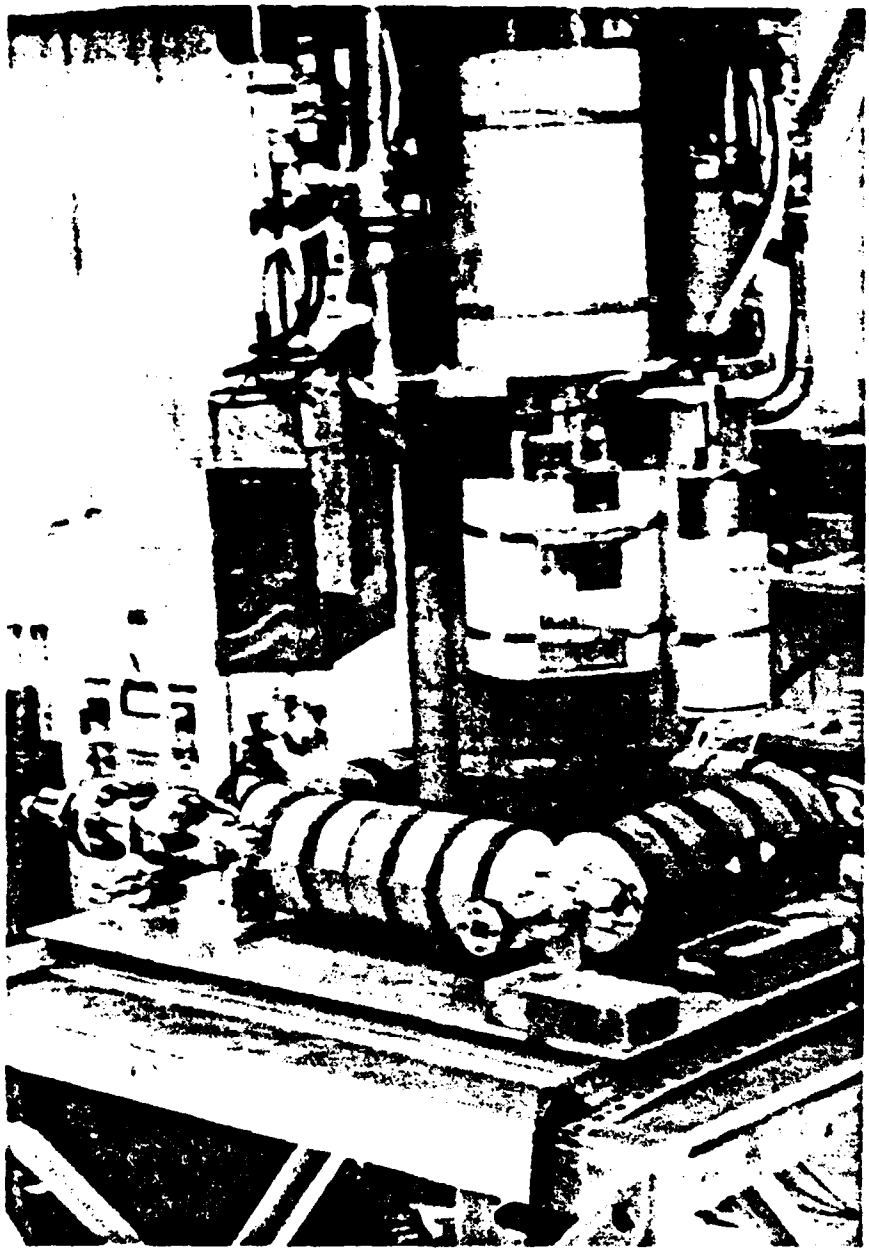

FIGURE 3.4. EXPERIMENTAL SET-UP

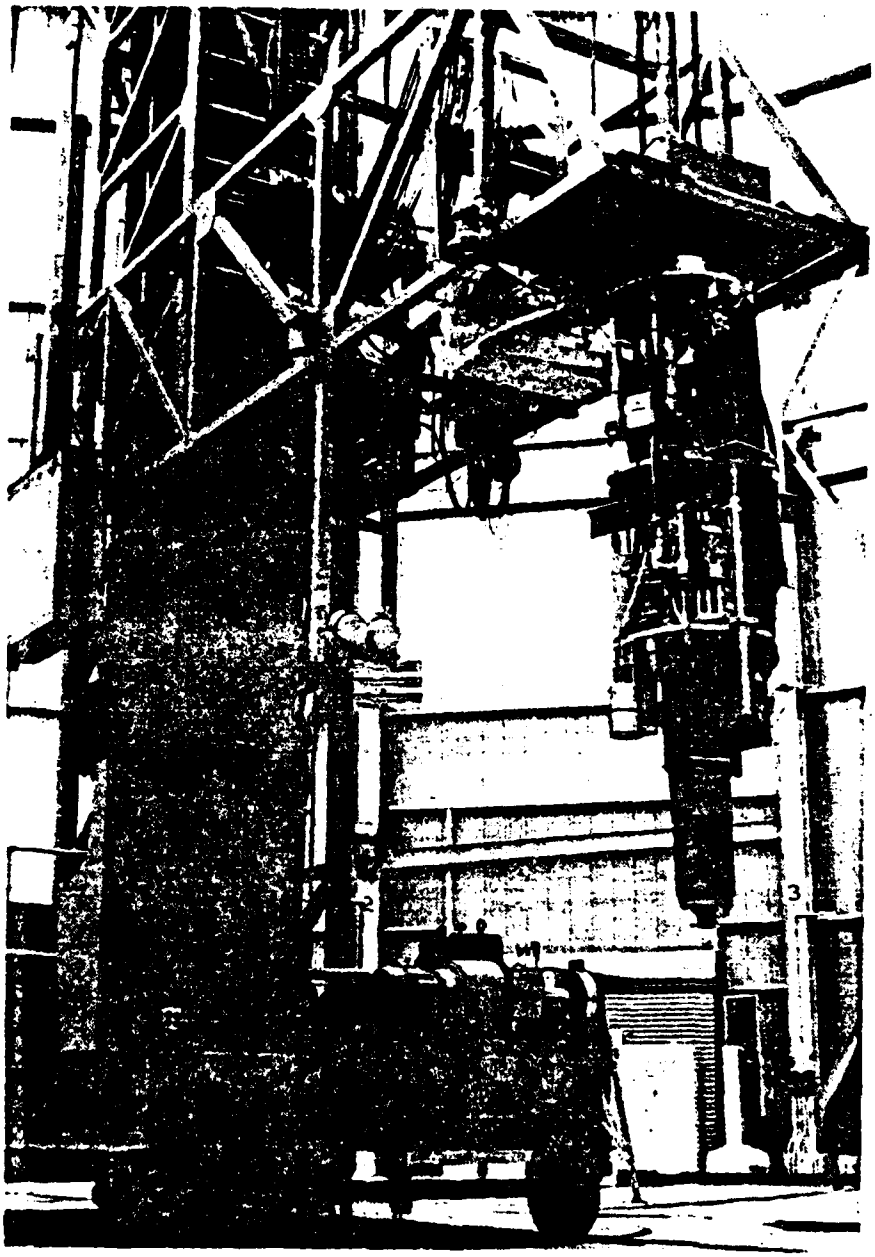

FIGURE 3.5. BURST REACTOR AND CRANE

6. The tubes were then removed from the LN_2 and allowed to return to room temperature. This increased the pressure in the flashlamps to 4.2 atmospheres.

3.2 SUPPORT EQUIPMENT

A gas handling system was designed to precision fill fluorine compounds under controlled temperature conditions (for example, crystalline XeF_2 has a partial pressure of 7 Torr at 90°F). Figure 3.6 shows the gas system as attached to the laser cavity. The SF_6 and XeF_2 containers are below the valve deck. All pump effluents are chemically treated for removal of all fluorine compounds, tritium (the by-product of ^3He fission) and other radioactive compounds.

For the second experimental series, the following modifications were made to the gas handling system.

1. The XeF_2 container was mounted directly on the laser chamber using a Varian extension and 2" valve. This was done to decrease distribution equilibrium time for this heavy gas.
2. A large bore diffusion pump was added to aid in decreasing cavity impurities and shorten cycle times.
3. A large amount of heat lamp and heat tape equipment was required in order to heat the cavity above ambient to avoid condensation of XeF_2. (Ambient ~50°F) For the first series of tests (Aug 80) ambient was 90°F.

Figure 3.7 shows the laser system as configured for the second series with heating systems installed. Before a series of tests, the total vacuum/pressure region was passivated for 24 hours using XeF_2 gas.

3.3 DIAGNOSTIC SYSTEMS

Two basic diagnostic systems were designed for the experimental

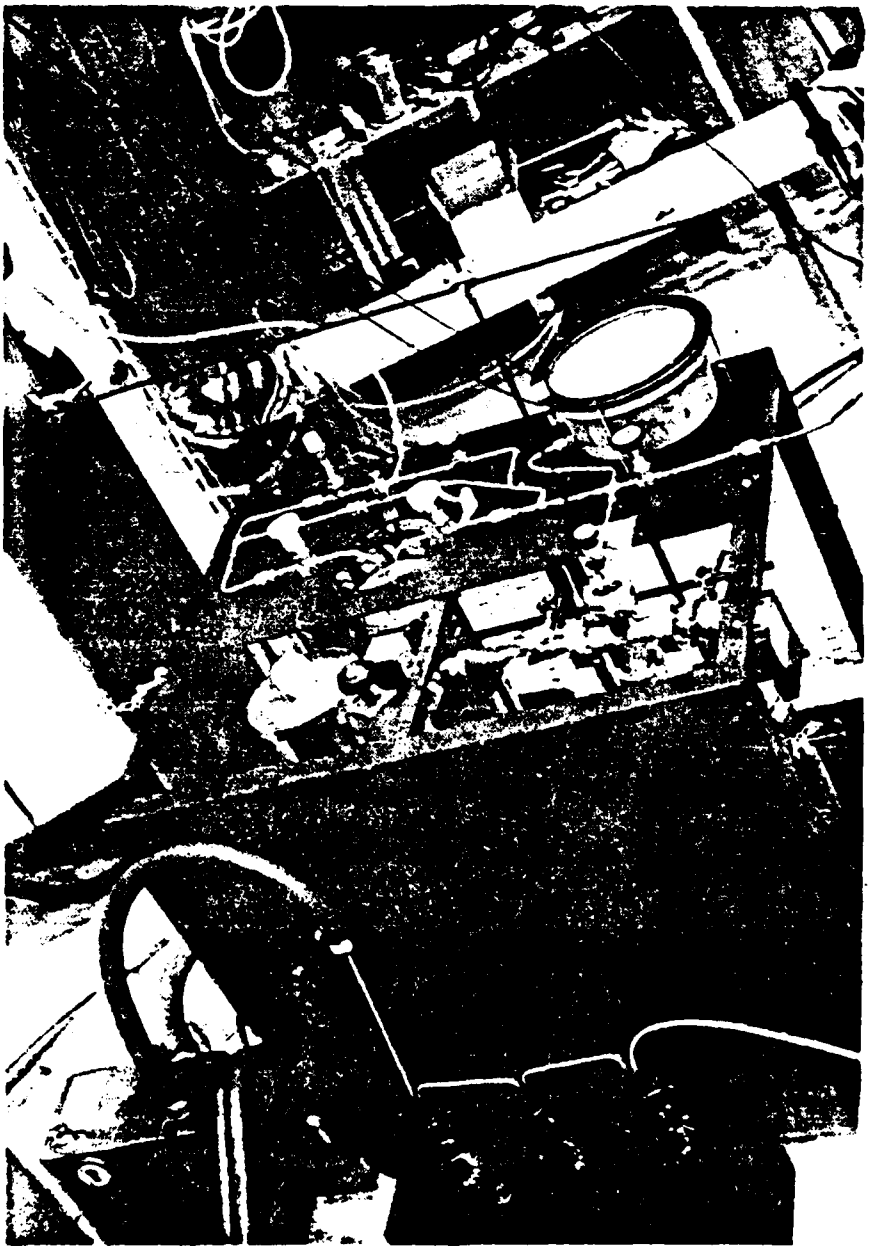

FIGURE 3.6. PUMPING STATION

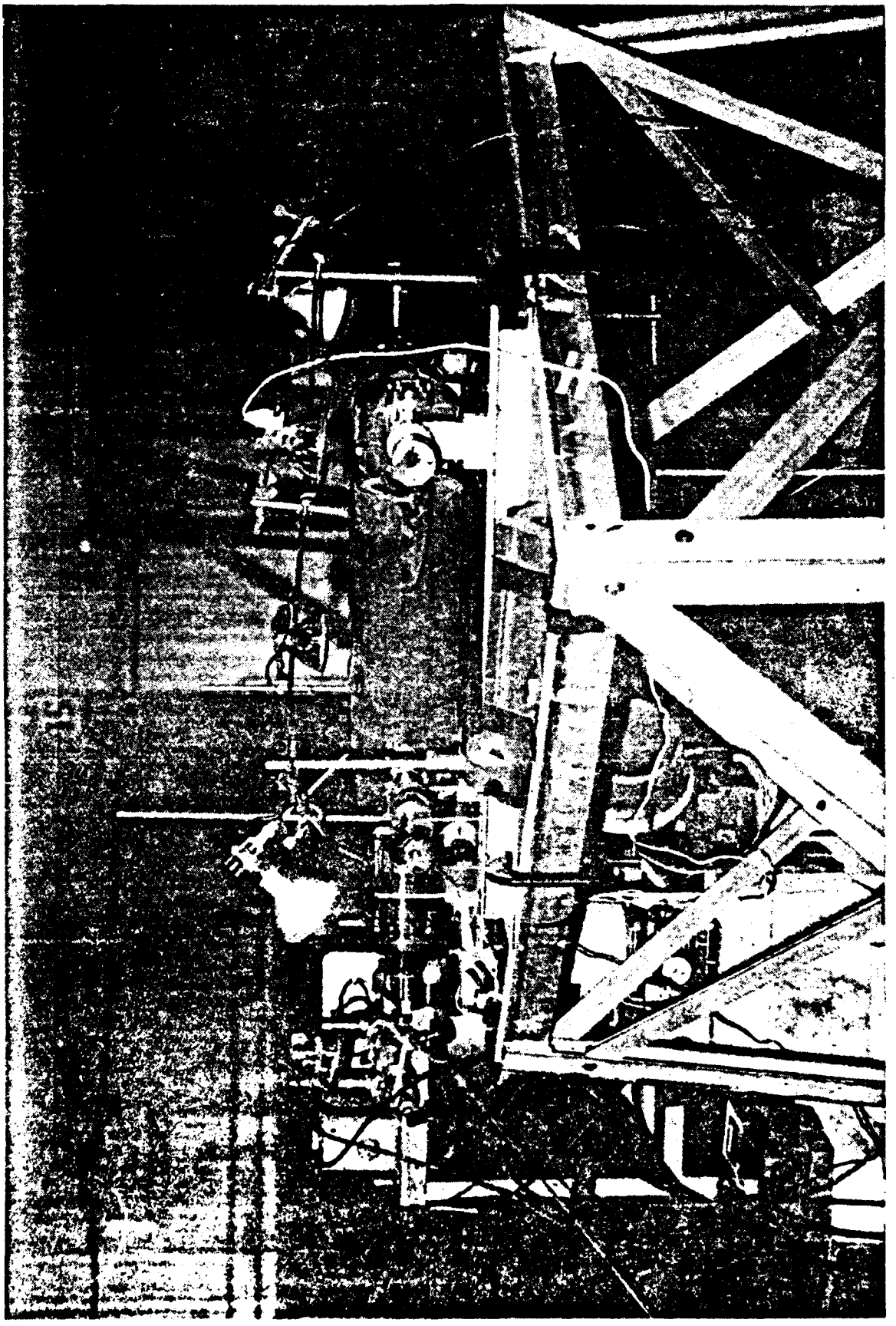

FIGURE 3.7. EXPERIMENTAL SET-UP SERIES 2

series: 1) Laser output spectroscopic analysis and 2) gain profile.

Alignment was performed using a 3 watt argon ion laser and an TN-1710 IDARRS optical channel analyzer. It provides both a spectroscopic profile and intensity analysis of the output beam. The TN-1710 was ttriggered by the reactor burst control and remained in the active mode during the reactor pulse.

The TN-1710 OMA was placed in a shielded position about 68 ft. from the exit aperture.

The gain profile was measured using the Argon ion laser as a probe and a fiber optic system (Dupont Pyfax) for transfer of the gain cell output to a photo-diode detector located in the control room area. Data was recorded by oscilloscopes. A TV camera with recorder viewed one of the observation ports. All optical paths were shielded from ambient air flow via sealed tubes in order to eliminate noise induced by dust particles. Both single line and differential gain measurements were made.

3.4 HARDWARE DISCREPANCIES AND CORRECTIVE MEASURES

Although results of the first series of reactor runs was productive, several hardware problems were discovered that impaired the initial goals of some of the diagnostic procedures.

1. The massive reactor crane structure when placed into burst position deformed the floor around the experiment stand so that the output beam was slightly deflected. This was not discovered until the second to last day of experimentation, with other effects (see #3) not allowing a repeat of the lasing experiments.
2. The mirror coatings on the exit mirrors were 99.7% reflective and not 98% as ordered and specified by the manufacturer. This was discovered during calibration and later verified by the mirror supplier as his error.

3. Laser mirrors were not fluoride resistant as ordered. Thus, upon exposure to atmosphere, they were damaged.

Corrective measures used in the second series of runs were 100% effective. First the laser system was located where the reactor could be inserted into the laser without leaving its turntable. This resulted in there being movement in the system. Second, a new set of mirrors that are insensitive to fluorine attack, with the proper reflectivities were used. A third problem, noisy output in the gain studies associated with a dusty environment was resolved by using a sealed laser path method.

In the second series of experiments, no significant hardware problems were encountered.

CHAPTER 4

4.0 EXPERIMENTAL RESULTS AND DATA ANALYSIS

In this chapter, analysis of the experimental data from the August 1980 and February 1981 series of tests is placed into three groups, 1) flashlamp characteristics, 2) gain measurements, and 3) lasing and fluorescence. Only a limited number of reactor shots were available. A significantly higher proportion of total shots (28) were dedicated to lasing (13) rather than to laser background assessment (7), gain (4), gain background assessment (2) and fluorescence (2).

4.1 Xe_2^* NUCLEAR FLASHLAMP CHARACTERISTICS

Spectroscopic analysis of the photon output obtained from the burst reactor experimental runs has provided evidence of an extremely large VUV band of radiation produced from nuclear excited Xe_2^*. Along with the VUV bans is a broad band continuum in the visible (and perhaps IR). Superimposed on this continuum are some large Xe Atomic line transitions. Table 4.1 shows the identified atomic and molecular transitions of Xe. Figure 4.1 shows the visible and IR spectral output of commercially available Xe flashlamps. High current devices (arcs) have a large blackbody continuum that peaks in the blue region superimposed with pressure broadened atomic line transitions. Many of these atomic lines which are quite strong at low current densities ($< 500 A/cm^2$) are almost completely obscured by the continuum at high current densities. The higher current density devices are the most efficient (~65%) in converting input energy to radiant energy in the visible ($.40\mu$ - $.90\mu$) (Goncz, 1966).

The data obtained from the initial series of experimental runs provided the most information about the nuclear excited Xe flashlamps. Figure 4.2 shows the spectral output of the flashlamp superimposed on the radiation

TABLE 4.1

Xe FLASHLAMP SPECTRAL EMISSIONS

(nm)	Species	Excitation Source		
		Arc	Discharge	Nuclear
172	Xe_2^*		X	X
461.1	XeII	X	X	X
467.1	XeI	X	X	X
484.4	XeII	X	X	X
487.6	XeII	X	X	X
492.0	XeII	X	X	X
504.4	XeII	X	X	X
534.0	XeII	X	X	?
542.0	XeII	X	X	?
609.5	XeII	X	X	?
823.0	XeI	X	X	X
835.0	XeI	X	X	?
882.0	XeI	X	X	?

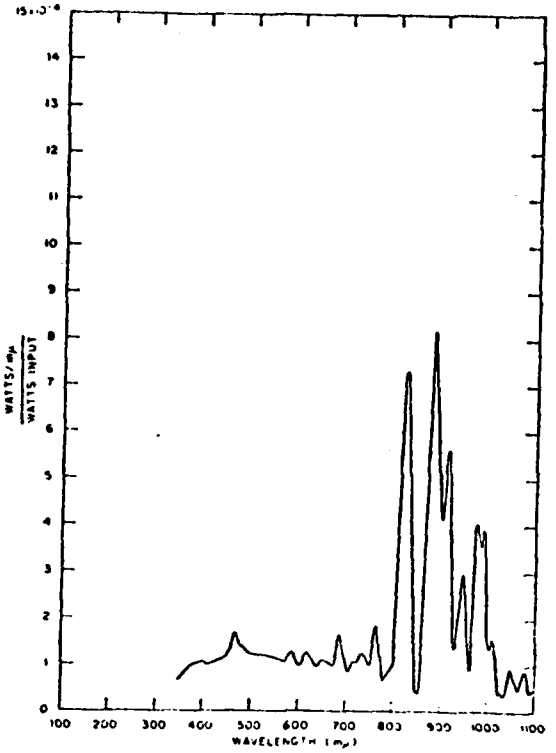

Spectral emission, experimental dc lamp (0.71-atm Xe, 0.41-atm Ar; 47 A/cm²), see also Table I. Spectral bandwidth equal to 10 mμ.

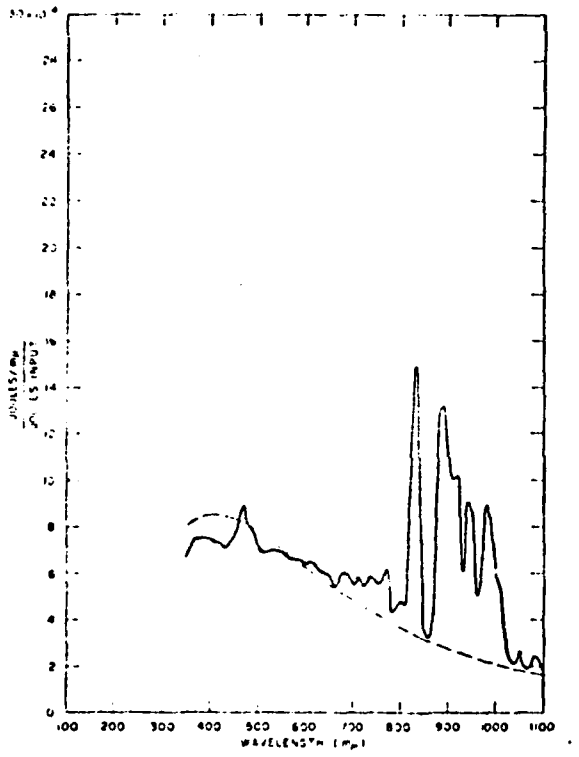

Spectral emission, FX-79 helical flashtube (0.26-atm Xe; 2870 A/cm², peak), see also Table I. Spectral bandwidth equal to 10 mμ. Broken line is relative spectral emission of a blackbody at 7100°K.

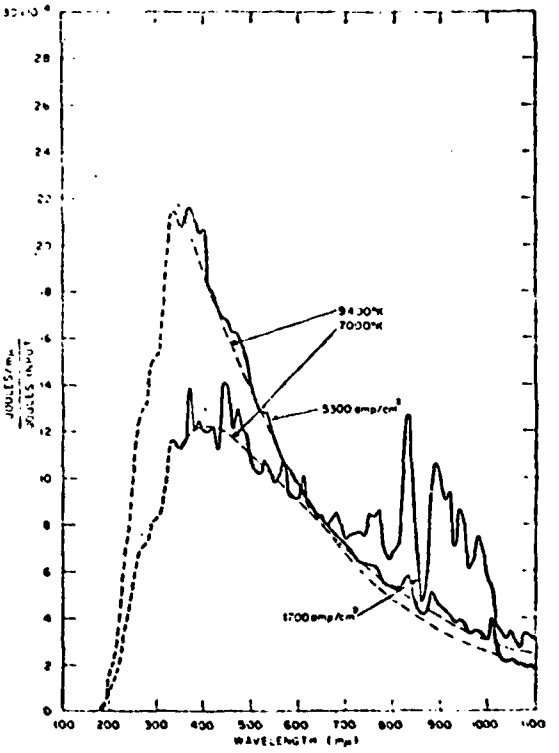

Spectral emission, FX-47A flashtube at two current densities (0.4-atm Xe; 1700 and 5300 A/cm²), see also Table I. Spectral bandwidth equal to 10 mμ. Coarse broken lines are relative spectral emission of blackbodies at 7000° and 9400°K. Fine broken lines represent measurements made in the ultraviolet and are not as accurate as those made in the visible and infrated.

FIGURE 4.1. SPECTRAL EMISSIONS OF COMMERCIALLY AVAILABLE Xe FLASHLAMPS

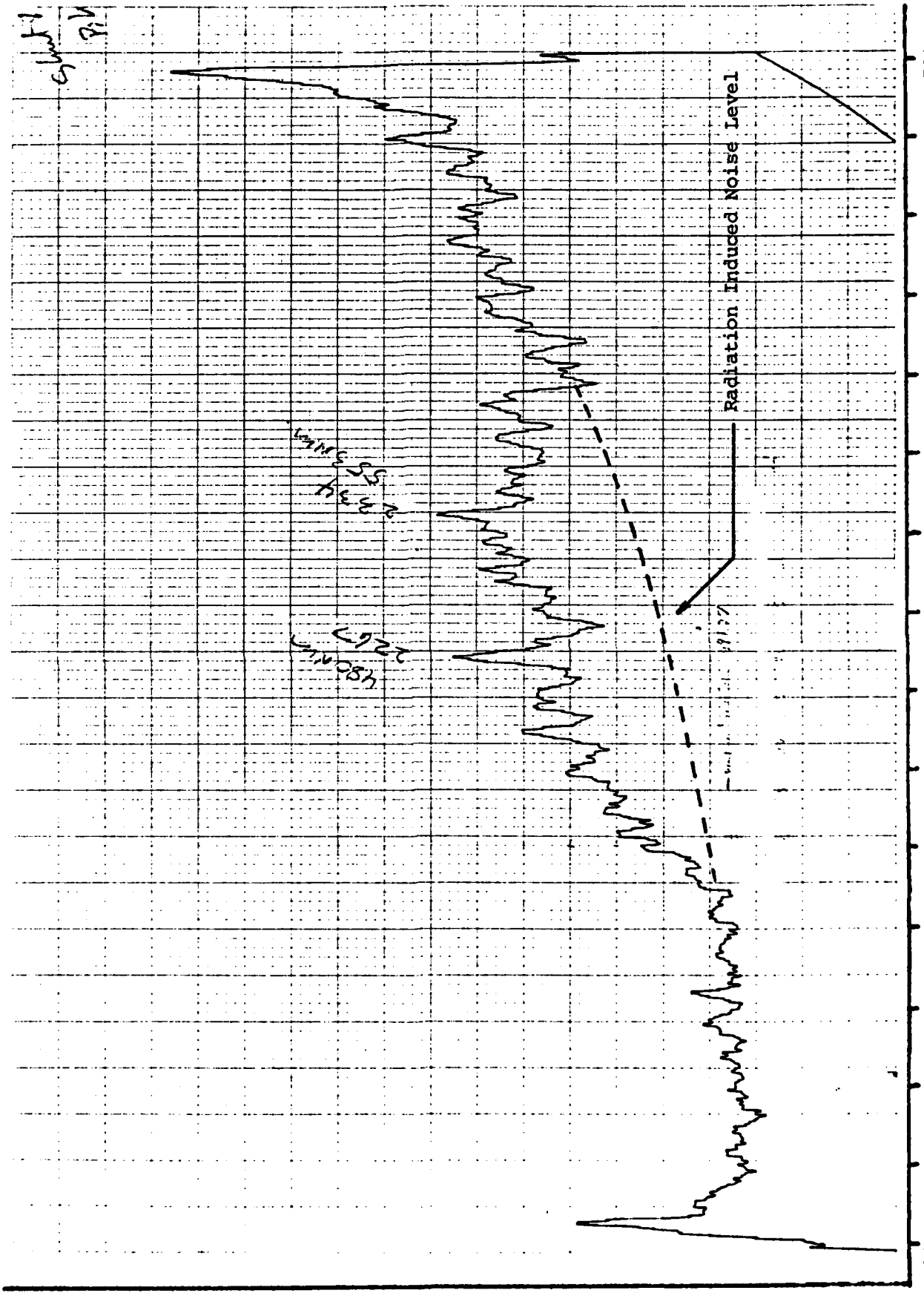

FIGURE 4.2. SPECTRAL EMISSION OF NUCLEAR EXCITED Xe FLASHLAMP

Figure 4.3 shows the VUV output of the flashlamp with the visible spectrum baffled. Figure 4.4 shows the time dependent intensity profile of the visible continuum. The VUV band appears at 175 nm as shown but it has been greatly attenuated by the air in the path to the spectrometer (~40 feet). A small visible continuum is shown with a few Xe atomic lines resembling that which is produced by the low current density Xe flashlamps. This is further verified by the presence of the very large red peak at 800 nm that is prominent with these devices.

After the first series of experimental runs at Aberdeen, an electric discharge excited Xe flashlamp (20 Kv, 1J pulse) was examined with the same detector (OMA).

Figure 4.5 shows the spectral output obtained. Note the attenuated VUV peak at 175 nm and the large blackbody continuum (7000°K) with the atomic lines superimposed. Many of these lines were observed in the nuclear flashlamp and the nuclear excited Xe irradiated at the UFTR (Walters 79). Although it appears that a nuclear excited Xe Plasma is much cooler with the electron temperature being near room temperature.

It has been shown by other NPL experimenters (DeYoung, 1978) that high pressure volumetric nuclear excitation has the same characteristics as the afterglow of an electrically generated plasma.

An unexplained phenomenon occurred during both series of experimental runs. When nitrogen was used as the buffer gas in the laser cavity the large VUV peak was observed but very little visible fluorescence was present. When SF_6 was used as the buffer gas, the VUV peak was diminished and several visible fluorescence peaks were observed. This phenomenon was repeated over several experimental runs.

During the first set of experimental runs spectra were obtained through a side viewing port. This exposed a section of the flashlamp to the solid

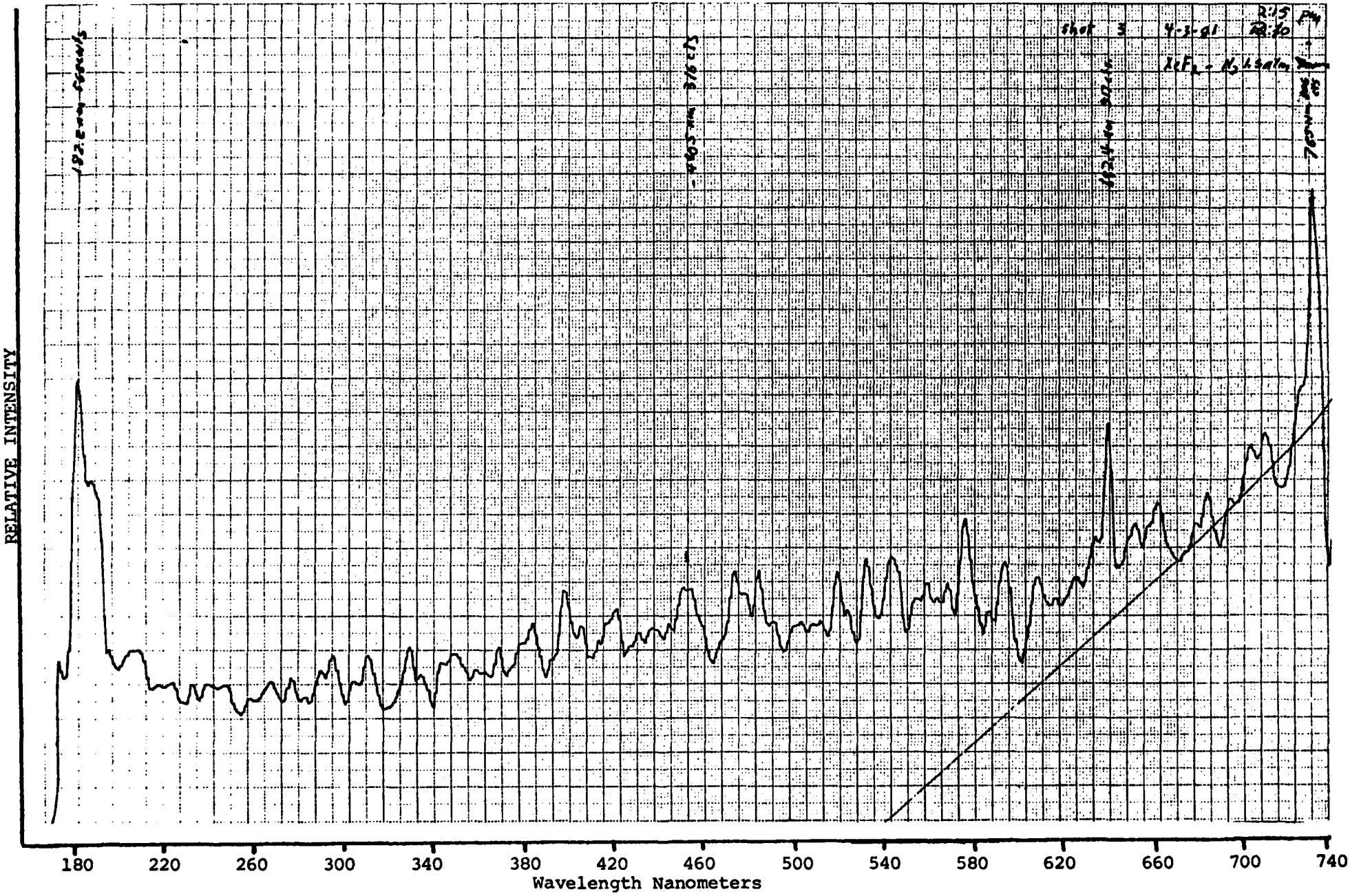

FIGURE 4.3. NUCLEAR FLASHLAMP SPECTRA WITH VISIBLE SPECTRUM BAFFLED.

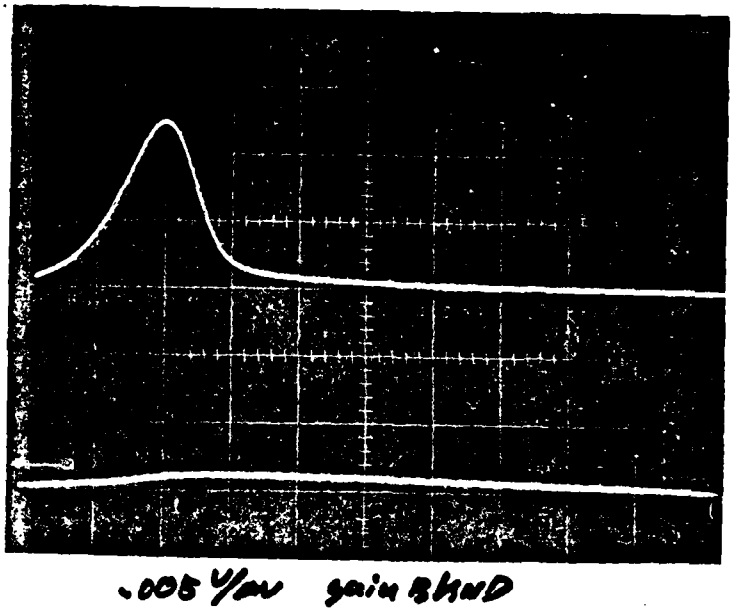

Photodiode
(fast neutron pulse)
5V/cm 50 μs/cm

Radiation Induced
Fluorescence (Fiber
Optic)
.005 V/cm 50 μs/cm

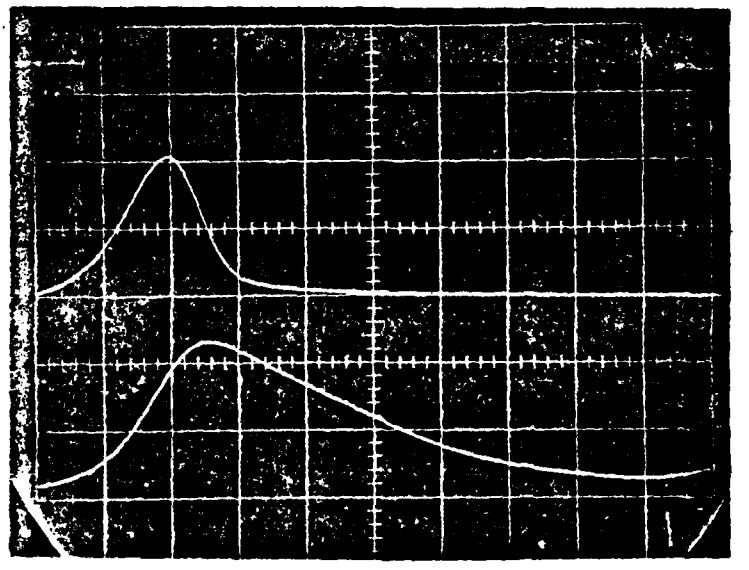

Photodiode
(fast neutron pulse)
5V/cm 50 μs/cm

Visible Continuun of
Nuclear Flashlamp
.005 V/cm 50 μs/cm
250 μs FWHM

FIGURE 4.4. TIME DEPENDENT INTENSITY PROFILE OF THE VISIBLE CONTINUUM.

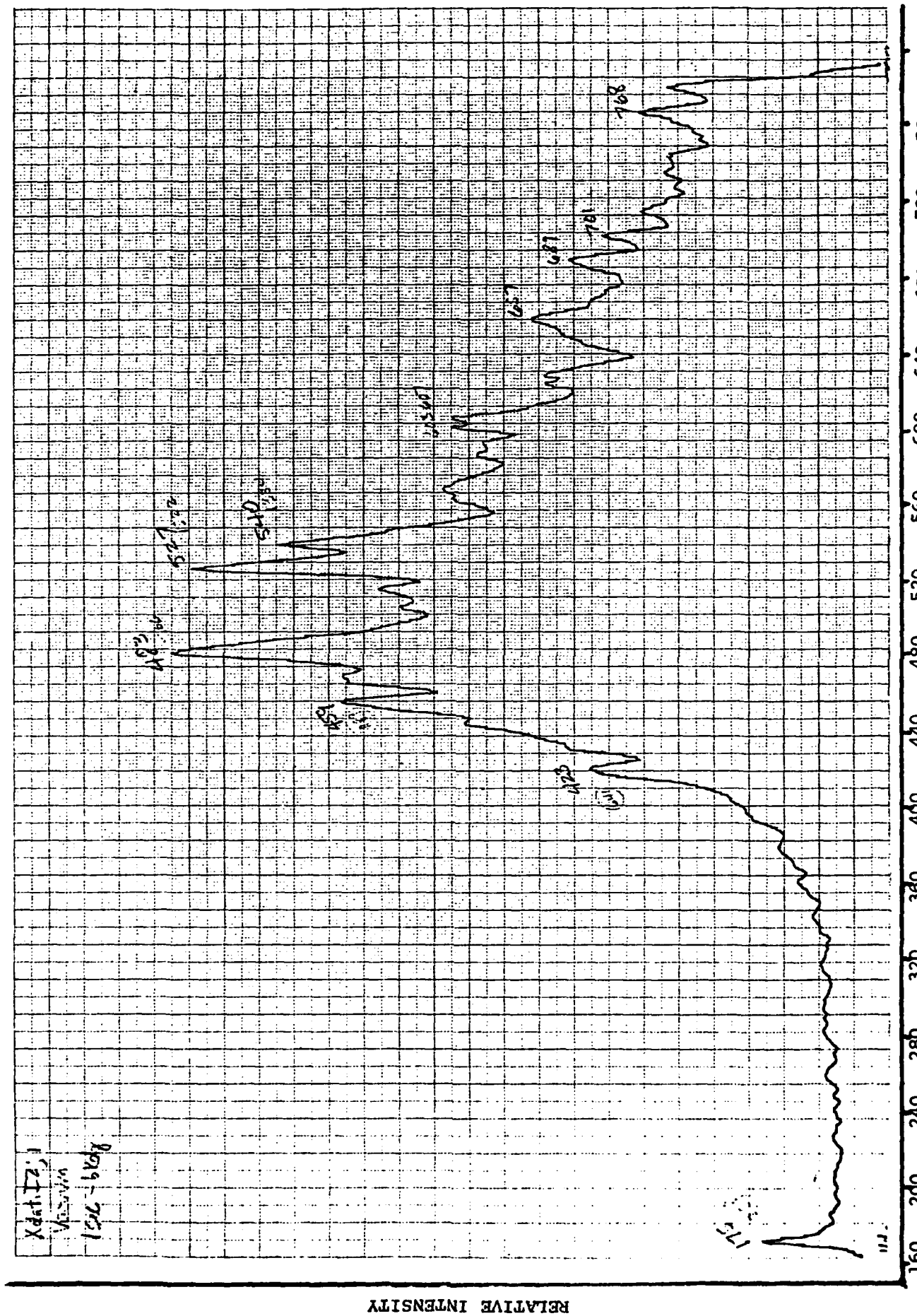

FIGURE 4.5. SPECTRA OF ELECTRIC DISCHARGE EXCITED Xe FLASHLAMP

angle viewed by the spectrometer enabling us to record the visible portion of the spectra emitted by the flashlamp. In the second series of runs spectra were obtained through the output coupler. This effectively baffled the visible output due to the geometry and mirror reflectivity in the visible. However, the VUV portion of the spectra is partially transmitted by the mirror resulting in the VUV peak observed during the nitrogen shots.

It is apparent from the literature on Xe flashlamps that flashlamps provide a spectral output that can be "tuned" from the VUV through the visible to the infrared. By varying in the current density or excited state density and the method of energy input (e.g., arc, discharge, nuclear) the spectral output is changed drastically.

The use of Xe flashlamps to photolytically pump laser systems has been demonstrated with VUV output as well as visible (blue). To utilize the nuclear excited Xe flashlamp to its fullest capability much more information about the efficiency and operating characteristics should be investigated. Since the hardware is available from this research effort, a detailed study of the spectral output in terms of energy transfer efficiency and spectral intensity should be undertaken. If the visible portion of the spectral output can be enhanced, many more nuclear excited photolytic laser systems are possible using this flashlamp. Perhaps Ar, Ne or Kr flashlamps can be made to pump other systems as well.

4.2 GAIN MEASUREMENTS

The burst reactor shots dedicated to gain studies are summarized in Table 4.2.

No significant gain was observed using both the OMA and differential measurements when the buffer was predominently N_2. When SF_6 was used as a buffer, gain was measured at 1%/meter with the differential diode system and 2.4%/meter with the OMA. Shot 14 verified that the fluorescence background measured by both the diode system and the OMA was an insignificant fraction of the probe laser input. Shot 14 also allowed for the calibration of the differential gain system.

If a gain of 1.5%/meter is assumed, the 1.8 meter (active region) laser cavity would require a cavity Q of 0.973 in order to reach threshold. Using the available mirrors, the maximum theoretical Q (perfect alignment) is 0.968. It is thus assumed that at least for the conditions of shot 15, lasing will not be possible at 488 nm.

In the second series of experiments, only one gain shot was obtained. It did not provide any significant data due to the unexpectedly high intensity level of the flashlamps at 488 nm providing an unworkable S/N level.

Even though two independent gain measurements were made in shot 15 with significant results, the low number of data points and the lack of positive proof of lasing led us to pronounce that the results of the gain studies are inconclusive.

TABLE 4.2

GAIN STUDIES

Series	Shot #	Gas Fill (torr)	Purpose	Diagnostics	Results
1	13 (1.2×10^{17} fis)	XeF_2 6 SF_6-23 N_2 1069	gain	OMA- laser on differential gain 4 pass cell	diff gain - 0.39%/meter noise dominated
	14 (1.10×10^{17} fis)	as above	background	OMA laser off differential gain 2 pass cell	insignificant fluorescence at 488 nm
	15 (1.15×10^{17} fis)	XeF_2 6 SF_6-1069	gain	OMA laser on differential gain 2 pass cell	diff. gain - 1%/meter OMA gain - 2.4%/meter
	16 (1.14×10^{17} fis)	XeF_2 6 SF_6-1070	gain	OMA laser on differential gain 2 pass cell	negative, loss of laser power at shot
2	9 (1.09×10^{17} fis)	XeF_2-5.5 SF_6-760	gain	single diode gain, 4 pass	no gain very low S/N
	10 (1.11×10^{17} fis)	vacuum	background	as above	large background

4.3 LASING AND FLUORESCENCE

In the first series of reactor shots, no indication of lasing was observed. The large 483 nm peak (Section 4.1) has been identified as an emission line of Xe. Originally it was thought to be associated with stimulated emission due to its being identical in structure to that of XeF(C-A) laser emission (untuned). Problems caused by nonfluorine resistant mirrors and platform movement (Ch. 3) would have made observation of lasing difficult if not impossible in this series of reactor shots. Measurements indicated inadequate gain for lasing but, due to inadequate data, not proof that lasing was impossible.

Table 4.3 displays the results of the lasing shots of the second series of reactor runs. Although no evidence of lasing was observed with the N_2 buffer, (shot 3) the SF_6 buffer system supplied very interesting results (shot 4). Figure 4.6 is a digitized subtraction of shots 4-2 where 370 and 460 nm lines are obviously above the noise. In subsequent shots when the system is unaligned, these did not appear. When aligned, they reappear although not as intense. The 460 nm output is not easily explained but may be the edge of the XeF(C-A) band or a Xe transition. The 370 nm band or line may be one of the following:

1. SIII lasing, = 370.0 nm, $4p^3D_2$-$3d^3P^o$

   via gamma and VUV dissociation and ionization of SF_6.

2. XeF^*(B-X) lasing with a nuclear induced shift to the red.

3. Lasing of SF_4 or SF_4^* + X → X^+ by photolysis of SF_6.

Number 2 above is highly unlikely, 3 is a possibility since SF_4 is polar and the second reaction is possible, but no backup information is available. Number 1 above has been observed (Cooper, 1965) in very low pressure SF_6 discharges as a predominant line. A preliminary calculation of the deposition of reactor gamma energy into the cavity has shown that an SIII population will appear with much more than adequate density to

TABLE 4.3

LASING STUDIES, SERIES 2

Shot #	Gas Fill (torr)	Purpose	Diagnostics	Results
^{1}(7.5x10^{16}fis)	Vacuum	Background Reactor Calibration	OMA	Background
^{2}(1.02x10^{17}fis)	Vacuum Post Passivation	Background Cavity Aligned	OMA	Background
^{3}(1.1x10^{17}fis)	N_2-1140 SF_6-50 XeF_2-5.5	Lasing Cavity Aligned	OMA	No Lasing VUV Band
^{4}(1.1x10^{17}fis)	SF_6-760 XeF_2-5.5	Lasing Cavity Aligned	OMA	No VUV Band 367 nm peak (± 11nm) 460 nm peak
^{5}(1.09x10^{17}fis)	SF_6-760 XeF_2-10	Unaligned Cavity Diagnostic	OMA	No Significant Output
^{6}(1.1x10^{17}fis)	SF_6-760 XeF_2-6.2	Lasing Cavity Aligned	OMA	365 nm peak 460 nm peak Others
^{7}(1.1x10^{17}fis)	SF_6-760 N_2- 5 XeF_2-760	Low Pressure Lasing Shot (Cavity Found Misaligned)	OMA	No Significant Results
^{8}(1.08x10^{17}fis)	SF_6-760 XeF_2-6	Lasing Shot	OMA	Small 370 nm

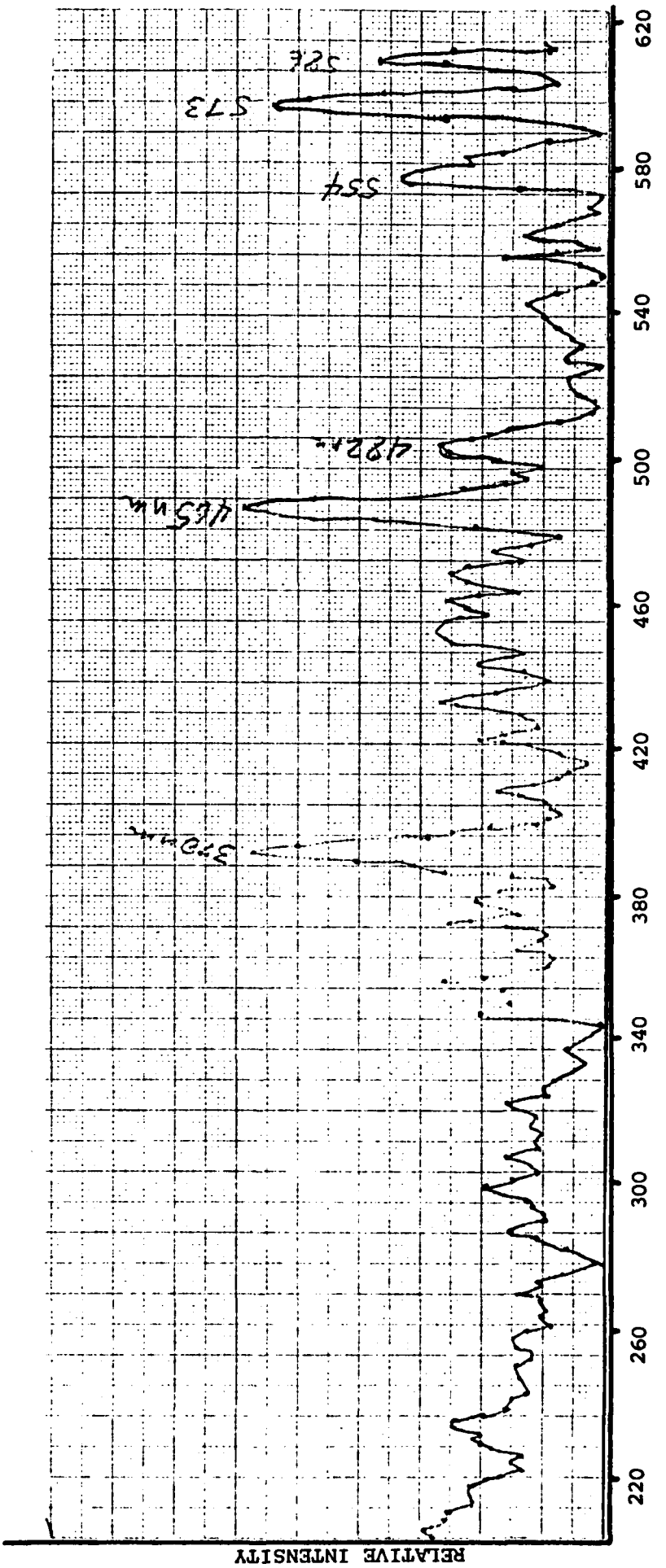

FIGURE 4.6. FLUORESCENCE FROM ALIGNED CAVITY BACKGROUND SUBTRACTED.

produce lasing; even considering that the cavity Q is only 0.1 at 370 nm. further investigation and firm calculations will be performed and reported at a later time.

It is evident that lasing of the XeF (C-A) transition was not observed nor was the flourescence from this band confirmed. But, if one assumes that the baffling is excellent, and shots 1 and 2 confirm this, and the output is only fluorescence, one can unfold the spectra through the mirror transmission and obtain the results shown in figure 4.7 for shot 8. In this case the background was arbitrarily set. The peaks were immediately identified with Xe flashlamp emission as noted in the associated table. This provides further proof of the intensity of the blue region flashlamp output and the difficulty of observing (C-A) fluorescence.

As mentioned in chapter 2, the cavity is extremely sensitive to intrinsic losses. In fact the cavity cannot sustain an intrinsic loss of 2×10^{-4}/cm and still achieve oscillation. If the intensity of the visible continuum from the Xe flashlamp is high enough to cause sufficient stimulated emission of XeF*(C) perpendicular to the lasing axis, the resulting loss of upper laser level density could produce an effective cavity loss greater than 10^{-4}/cm and prevent lasing action.

Figure 4.8 shows the stimulated emission cross section as a function of wavelength measured by SRI (Bischel, 1979). As shown the cross section peaks in the blue at about 480 nm. This corresponds to the peak output of the visible portion of the Xe flashlamp emission. In fact the two curves overlap considerably.

The rough calculations presented below indicate that the visible portion of the nuclear excited flashlamp could produce enough stimulated emission perpendicular to the lasing axis to create a substantial loss of XeF(C) state. The visible output of the nuclear excited flashlamp has not been calibrated.

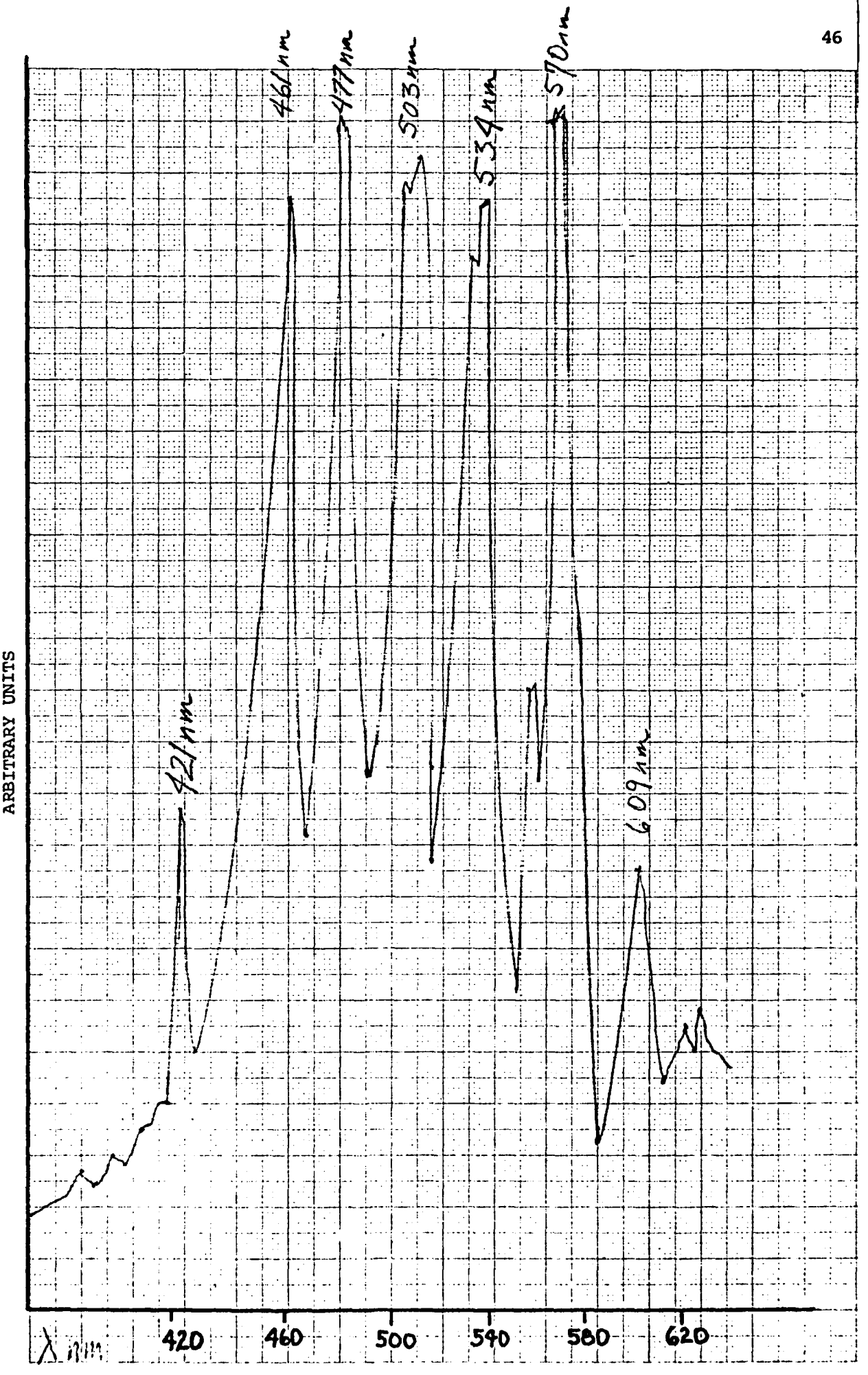

FIGURE 4.7. FLASHLAMP SPECTRA UNFOLDED FROM MIRROR REFLECTIVITY (Bkgd Subtracted)

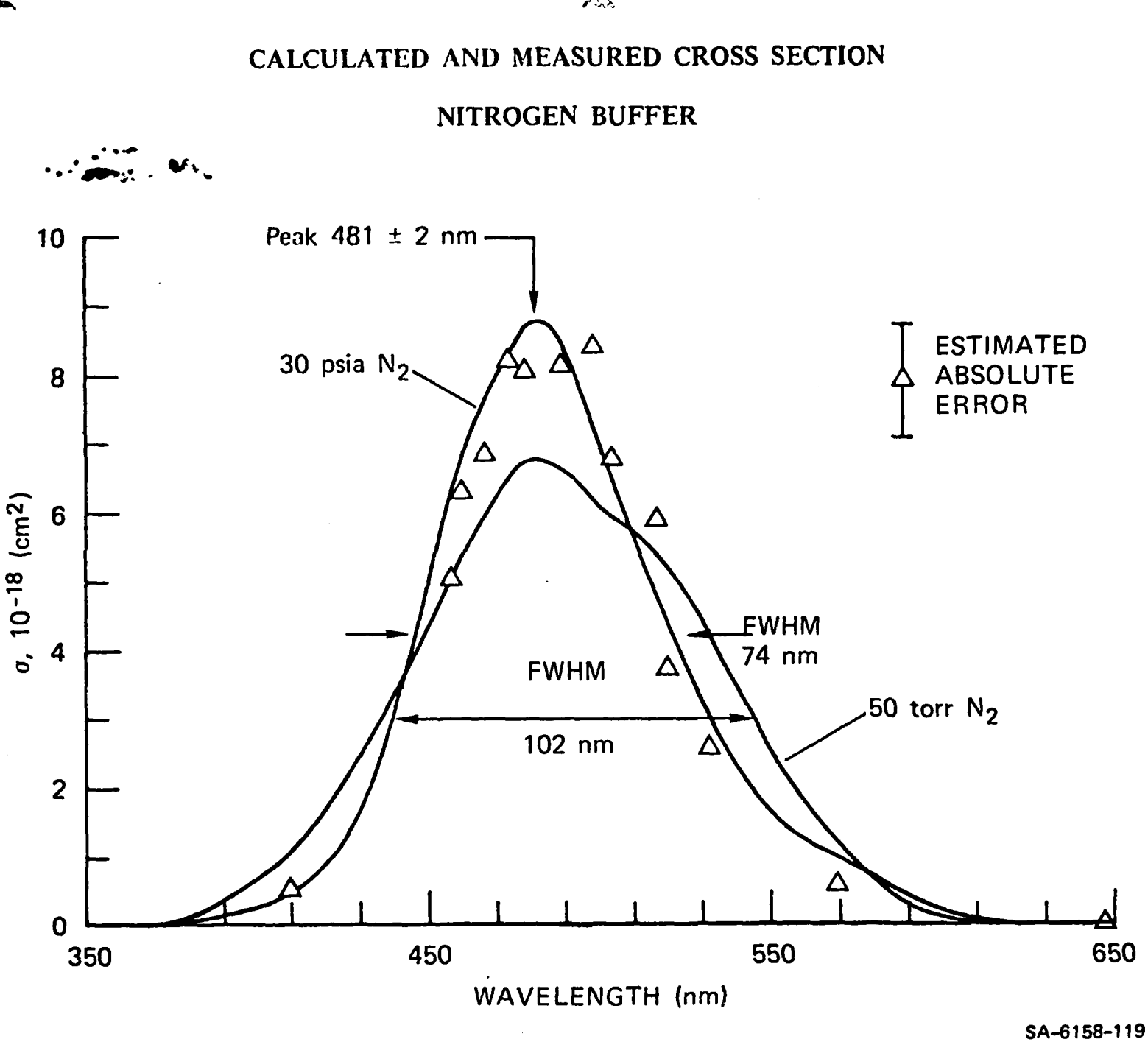

FIGURE 4.8. SRI DATA

However, it can be assumed that at least 1% of the total radiant energy released by the flashlamp is in the visible. Since only 50% of the input energy can be accounted for in the VUV, as much as 40% of the input energy could be released in the visible with the remaining 10% lost in the walls.

C State Removal Calculations

$$\text{Peak VUV photon flux} \approx 2 \times 10^{21}/\text{cm}^2\text{sec.} \quad \text{(Lim,1981)}$$

$$\text{Peak visible photon flux} \approx (1\%/50\%) \times (480\text{nm}/170\text{nm}) \times (2 \times 10^{21}/\text{cm}^2\text{sec})$$

$$\phi_{vis} \approx 1.1 \times 10^{20}/\text{cm}^2\text{sec}$$

$$\text{Removal rate of XeF(C)} \approx \phi_{vis} \cdot \bar{N}\,(\text{XeF C}) \cdot \sigma_{se}\ (\text{cm}^2)$$

$$\approx (1.1 \times 10^{20}) \times (1 \times 10^{13}) \times (3 \times 10^{-18})$$

$$\approx 3.3 \times 10^{15}/\text{cm}^3\text{sec}$$

This term should be added to the rate equations for the XeF (C) state population once $\phi_{vis}(t)$ has been measured. If the blue region emission turns out to be a substantial portion of the imput energy ($\geq$ 10%) then photolytic pumping of XeF (C) will require a modification of the flashlamp design to filter out the visible portion of the spectral emission. For this effect, which has not been identified in the general literature, we will coin the phrase "Parasitic Amplification".

It should be evident that the nuclear pumped flashlamp cannot be modeled in the identical manner to electron beam flashlamp systems. The parasitic amplification term although present may not be significant in, for example, the SRI experiments. This is because all kinetic processes governing the formation of XeF (C) population are short term i.e. < 100 ns. In the e-beam systems the pump pulse "switches" to a maximum level and remains there for 1 microsec. Lasing builds up quickly (30 ns) but decays after 200 ns due to XeF_2 depletion and now perhaps parasitic amplification. In the nuclear pumped

flashlamp case, the pump pulse exponentially rises over a 60 microsec. period until the peak population is reached. Two important differences exist between these two systems:

1. The e-beam laser is not in equilibrium with the pump pulse. All kinetic processes are driven by the source pulse shape and fast changing plasma populations. In the nuclear flashlamp case, the system is in secular equilibrium with the pump pulse. That is the fast kinetics of the laser are driven only by a slowly varying quasi-CW source term, a result of low specific input. Almost no energy (<1j) is deposited into the XeF_2 cavity before the population of XeF (C) has peaked ($\sim 10^{14}$). Integrated over the total input pulse, the parasitic amplification term may have even a larger effect in the e-beam excited case than the nuclear case, if we assume that the flashlamps are identical in spectral output distribution. Since the e-beam system is far above threshold, the photon flux extracting energy in the axial direction far exceeds that in the radial direction and thus the laser output (loss from the system) term predominates. In the nuclear flashlamp case much energy is deposited before the peak XeF (C) population is obtained ($\sim 10^{13}$) thus the depopulation due to parasitic amplification is a CW effect depending only on the input levels. Since the population is barely above threshold, the same percentage loss as in the e-beam case will drop the system below threshold.

2. In the e-beam case, only 12j of energy is deposited in a 1 meter flashlamp. The nuclear flashlamp absorbs 250j over the same length tube. In the time frame of collisional thermalization, the low input e-beam system may not produce the Xe blue continuum and only display recombination radiation because the plasma produced is of the (cold) recombination type. This is similar to an afterglow. In the nuclear flashlamp we have observed the Xe continuum. Thus we expect the blue region fluorescence to be considerably enhanced per input joule over that of the e-beam case. This could be more than an order of magnitude greater. Thus, parasitic amplification becomes a significant loss term.

It is evident that the low gain measured in the first series is a result, at least in part, of the mitigating effects of parasitic amplification. Parasitic amplification may also be in part responsible for the differences between the calculated and actual system efficiency in the e-beam excited photolytic XeF (C) lasers.

CHAPTER 5

5.0 CONCLUSIONS AND RECOMMENDATIONS

It is evident from the data obtained in this research effort that high power lasing was not obtained. Nevertheless, from the same data, much has been learned and much has yet to be explained. Perhaps more new questions have arisen than answers given.

Several facts have been established:

1. The VUV output of the Xenon flashlamps, Xe_2^*, is extremely large.

2. The visible region (mostly blue) output of the flashlamps is also very large; in fact, much larger than expected from previous data and other results. This provided a difficult environment for spectroscopic analysis of XeF(C-A) fluorescence and gain studies. Since 40 to 50% of the flashlamp energy must be removed by processes other than Xe_2^* emission, several hundred joules must be accounted for by other fluorescence, thermal heating and wall losses. The majority of this energy will be lost via the traditional Xe blue region fluorescence. Other experimenters did not view a large visible continuum and Xe^* structure due to a unique set of view angles, experiment construction and energy considerations. Essentially, the signal to noise ratio of this experiment in comparison to the SRI work (defined as $XeF^*(C-A)/Xe^*(483nm)$) is depressed by at least 2 orders of magnitude.

3. The SF_6 buffer eliminates the Xe_2^* 172 nm output observed with N_2 as a buffer.

4. A 370 nm line or band from the SF_6 buffer system has been viewed at an intensity far above fluorescence levels for any component and only

when the laser cavity was aligned. This has been attributed to one of the following:

a. Lasing of SIII, λ = 370.9 nm, $4p^3D_2$-$3d^3P^o$, via gamma and VUV dissociation and ionization of SF_6 (high probability explanation).

b. XeF^* (B-X) lasing with a nuclear induced shift to the red from 353 nm. (probably not possible).

c. Lasing of SF_4 or $SF_4^+ + X \rightarrow X^+$ by photolysis of SF_6 (unknown probability).

Perhaps the most important result of this research is the knowledge of how to build nuclear flashlamp laser systems and the applicability of certain alternate designs that will allow the injection of more energy into the active region.

In this chapter, the results of this research are reviewed, alternate experimental designs and alternate XeF_2 fueled laser candidates are explained and other nuclear pumped laser systems that are deemed most promising as a result of this research are presented.

5.1 SUMMARY OF EXPERIMENTAL RESULTS

The first series of reactor experiments, although flawed by unexpected floor movement and inappropriate mirror coatings, established that the VUV emission from the nuclear flashlamps was indeed as strong as anticipated. What was not expected was the ability to observe this emission peak. (The red end of the band at 185 nm) with the optical multichannel analyzer. Upon analysis, the measured levels indicate that from the megawatt output peak generated during a burst, approximately 12 orders of magnitude absorption exist from the flashlamps to the OMA. This is reasonable. Also, it should be noted that the OMA has been sensitized to the VUV via a fluorescent coating. When the buffer gas was pure SF_6, the Xe_2^* band was not observed. The experimental runs of the second series verified these results. This indi-

cates a possible high level of absorption by SF_6 of the 172 nm band and perhaps an energy transfer to XeF_2. The reaction $SF_6 + VUV \rightarrow SF_4$ may account for the absorption. An additional unusual event is the fact that under vacuum conditions, the VUV band is not observed. 1) Does N_2 act as scatterer allowing a portion of the VUV to exit the output window and SF_6 does not scatter?; 2) does XeF_2 scatter the VUV and SF_6 is a heavy absorber in that region?; 3) Is there an extremely large emission band of N_2 or N_2^+ at 185 nm? Not likely, none has ever been measured. The most plausible conclusion could be number 2 above, but at this time the answer is not certain.

The large visible region output from Xe was not expected due to information from other experiments (SRI, 1980) and previous research (Walters, 1979). But if sufficient energy is deposited over a lengthy period of time, the recombination and collision excited Xe system will fluoresce with considerable output as expected from any Xe flashlamp. The ratio (S/N) of $XeF^*(C-A)/Xe^*$(482 nm) increases with increased energy input rate. Due to quenching by XeF_2 of $XeF^*[C]$, the faster the removal of XeF_2 by photolysis, the higher the population of $XeF^*[C]$. It is expected that the characteristics of all high energy charged particle excited flashlamps are similar, but in the SRI experiment, 12j of energy was deposited in 1 μs providing at 50% efficiency, a VUV photon input of 6×10^6 watts. In the nuclear pumped case ~1 kj was deposited over 200 μs. At 50% efficiency this provides an average input of 3.75×10^6 watts. In the nuclear case, the lasing output relys on burning out the XeF_2 in a bleaching wave effect until the "right" environment is reached at the center point where $XeF^*[C]$ population is adequate for lasing (~20-50 μs). But this is never as high as it is in the SRI experiment. During this period, collisional excitation of Xe by secondaries and recombination has transferred energy to Xe^*

fluorescence in the blue region (~40% of total). Furthermore, the inside of the containment is highly reflective in the blue. Thus, the nuclear flashlamp is an excellent VUV source but also an excellent blue region flashlamp. It only becomes a good VUV pump source when the kinetics of the absorbing system are within an order of magnitude of the pump source, unless, of course, the flashlamp is overpowering. The decrease in XeF(C-A) S/N of the nuclear pumped case over the e-beam case is estimated to be about a factor of 200.

In the first series of experiments, the extremely bright Xe^* output was viewed due to inadequate baffling. This was corrected in the second series. Because of this baffling problem, the 480 nm (483 nm Xe) band output was originally thought to be XeF(C-A) stimulated emission since its structure was (unfolded through the 99.7% mirror) identical in all respects to the spectral output of the XeF(C-A) laser (SRI 1980). Further flashlamp research led us to correct this observation and attribute this output to the very intense 482 nm Xe fluorescence line.

The gain measurements of the first series of experiments were obtained by a differential method. The N_2-SF_6-XeF_2 mixture provided a gain of 0.39%/meter, insignificant in the noise background. A gain of 1 to 2.2%/meter was measured using the SF_6 buffer. This is considered a firm data point. The single gain shot in the second series of experiments was inconclusive due to a large background from the flashlamps. This problem was mitigated in the first series by the distant placement of sensing aperture but in this case measurements were difficult due to a large dust generated noise environment. As a result of the analysis of all data, gain at 488 nm is considered possible. But, of course, in the range of 1-2.4%/meter (SF_6) results are inconclusive due to an inadequate volume of data. Assuming a 1.5%/meter gain,

cavity Q requirements would be .973. Since the best cavity available was .968, lasing is not expected from XeF^*(C-A) in this experimental system. Again, the results point out that SF_6 may be a superior buffer in slow pump rate XeF_2 photalytic systems.

In the second series of experiments, only 9 shots were available. Three bursts were used for background assessment. As a result, it was determined that the Xe spectrum was effectively baffled around 480 nm from input to the OMA. The first data shot using the N_2 buffer showed only the VUV output from the flashlamps with no indication of lasing output. In the next shot where all physical conditions remained the same (alignment untouched, temperature identical) the VUV spectra disappeared and a large line appeared at 370 nm. This line was attributed to lasing from gamma photolysized and double ionized sulphur (from SF_6), a shift of the XeF(B-X) system (highly unlikely) or a mechanism involving SF_6 photolysis to SF_4 producing the output.

Most interesting was the disappearance of this line in the subsequent unaligned cavity shot and its reappearance again upon alignment (although at a lower output level).

5.3 ALTERNATE XeF_2 EXPERIMENT DESIGNS

Since the results of the flashlamp tests indicate a significant visible region output not observed in the CW studies (Walters 1979) it would be prudent to experimentally measure the output in the various bands using absolute techniques. This can be done by various methods using the burst reactor and sections of the present experiment. Since at least 6 flashlamps are available, statistically accurate data could be obtained.

An alternate design for the XeF_2 photolytic laser (or any photolytic laser) should be considered. The following design was initially proposed but not implemented due to the unavailability of certain components and the cost of their development. Several of these are now available.

The design consists of a rectangular box of about 40 x 7 x 0.7 cm. 99.7% reflective mirrors at 480 nm are placed at two of the 7 cm ends. The large side walls are of sapphire or suprasil sheet with support spacers placed between the sheets (0.7 cm spacing). On the outside of these sheets is placed the flashlamp chamber, a VUV mirror and moderator/flux trap. The flashlamp need not extend to the side mirrors. Output sections are placed on the mirrored ends in alternate positions. External or internal mirrors can be used. A bellows arrangement will allow adjustment of the path length or number of internal bounces in the cavity. A small (25 mW) air cooled argon ion laser will be placed intracavity to assure alignment of the system. Although the output beam diameter will be severely restricted by the small Ar^+ laser bore, proper cavity design will not alter the lasing threshold point from its norm. Note that with only a 30 cm active bleaching wave driven region, 7 reflection lengths will exceed the present cavity's length. This is easily accomplished in this system while maintaining a high Q cavity. Although the Ar^+ laser is commercially available, minor modifications are required for this design. The 30 x 7 cm suprasil sheets would be special order components. All other parts are now standard. This is an expensive design but should be considered for future work in XeF_2 photolysis laser systems. Gamma pumped liquid Xe flashlamp systems could also be accommodated by a double wall version of this design.

5.4 ALTERNATIVE NUCLEAR PUMPED EXCIMER LASER SYSTEMS

Excimer laser systems have proven to be some of the most efficient and highest power laser systems to date. However, due to their nature (i.e., short lifetimes and UV or visible laser transitions), the pumping power required to reach threshold (see Chapter 2) is very high (on the order of MW/cm^3).

In the photolytically driven excimer laser system a penalty must be paid in terms of the pumping power due to geometrical considerations. This

results in almost an order of magnitude loss of power density in the pump pulse. Although the energy has been "cleaned up" mitigating nuclear induced effects, the loss in power density may be more critical than any nuclear considerations.

Direct nuclear pumping of XeF^* excimer lasers has been investigated by us in conjunction with Fisher and Lim at Wayne State University. It has become evident from examining the necessary conditions for lasing that a pump pulse of shorter rise time and higher peak power density is required than is available with the present systems utilizing the Fast Burst Reactor.

Analysis of the direct nuclear pumping of XeF^* was done by comparison of two different fluorine donors. The first case is the $Xe:Ar:NF_2$ system that has successfully demonstrated lasing of XeF^* from discharge and e-beam pumping. The second case is the $He^3:Ne;XeF_2$ system. To date no XeF^* laser system has been demonstrated using XeF_2 as a fluorine donor except for the photolytic system.

For a given energy input to the $Xe:Ar:NF_3$ system, the pump pulse must produce enough Xe ions or excited states to reach threshold before sufficient NF_3 has been dissociated to prevent lasing. This system works nicely for MW/cm^3 pulses of submicrosecond duration. The difficulty of nuclear pumping this system is evident in the long pump pulses that are produced with the present nuclear source technology. There are other factors such as the buildup of NF_2 and other quenching agents that make nuclear excitation of an NF_3 bearing system unattractive.

In the case where XeF_2 is used as a fluorine donor, the long pump pulses found in the nuclear systems are more favorable. XeF_2 can be dissociated by electron attachment to form $XeF + F$ or $Xe^+ + F + F$ (Sides, 1976). In either case, XeF^* can be produced by direct nuclear excitation. Since XeF_2 is a severe quencher of XeF^* the optimum lasing condition will be ob-

tained late in the pump pulse when most of the XeF_2 has been dissociated to 1) provide XeF^* and 2) atomic fluorine for the formation of XeF^* when combined with Xe ions. This is in direct contrast with the NF_3 case where the conditions for lasing get worse with time as the NF_3 is consumed. For long pump pulse sources such as in nuclear pumping, a XeF_2 direct pump system may provide a suitable environment for an excimer laser.

5.5 OTHER NUCLEAR FLASHLAMP SYSTEMS

It is evident from this research that an effective blue region nuclear flashlamp has been generated. As mentioned previously, calibration of its efficiency is required. With the addition of a surface coating or gas additive for wavelength shifting, most of the VUV energy could be converted to the blue region. Even without these changes, the present flashlamp system with its reflective casing could be used in the photalysis of CF_3I, IBr or C_3F_7I to produce 1.3 μm output from the I^* product. The upper state lifetime is in the millisecond region. Thus, total reactor energy deposition can occur before the onset of lasing if the cavity Q can be depressed until the lasing point and parasitic oscillations (to the side) are avoided. An initial attempt at CF_3I,I^* lasing was attempted by Fuller (U of F, unpublished) in 1974 at the SPR-3 Sandia burst reactor. It was a direct pumped ^3He device. Results were negative because no gas purification systems were used. This result could be expected because even flashlamp pumping of this system was not successful. For such iodine systems, gas purity is of paramount importance. The present system has been developed to provide this environment.

A $Nd:POCl_3$ liquid laser may be easily pumped with the energy available from a nuclear flashlamp assuming it isn't more profitable to directly gamma pump this system (see next section). Liquid systems should not suffer the damage problems that were observed in early gamma pumped

solid laser experiments.

5.6 LIQUID NUCLEAR PUMPED LASER SYSTEMS

The most advantageous liquid system for nuclear pumping is phosphoral chloride with neodynium in the +3 valence state. U^{235} can also be added in the +3 state producing the combination U^{3+}:Nd^{3+}:$POCl_3$. The chemistry and lasing capability of this system has been investigated thoroughly (Samelson, AD-787895) with flashlamp pumping extending power to 400 watts average at 2% efficiency. 1 kw average power is expected. Power and repetition rates of this pulsed system were limited by flashlamp sources and the non homogeniety of pumping via external photon flux deposition.

Recent work (Bondareu, 1976) utilizing Nd^{3+}:PBr_3: $AlBr_3$:$SbBr_3$ has shown great promise as a more efficient and safer chemistry system. Some variations of the chemistry may provide an excellent medium for liquid nuclear pumped laser systems (LNPL).

The advantages of LNPL systems over traditional liquid and other nuclear pumped systems are:

a. Homogeneous pumping

b. Small size (laser and reactor could be the same liquid)

c. High energy density

d. Flow cooling

e. Variable wavelength capability (other than 1.05 μm, Nd^{3+})

Mechanisms for pumping Nd^{3+} or any of the other rare earth elements (U^{3+},2.513 ; Eu^{3+},0.611 : Table 5.1) rely on high energy injection and energy cascade to excitation levels that are equivalent to nonradiative absorption bands leading to the excitation of the rare earth element. Figure 5.1 shows the transitions and energy level diagrams of the U^{3+} ion in CaF_2. Note that the transitions to the laser upper/state are non-radiative from $4I_{1/2}{}^3$ states and the continum. Most rare earth systems

TABLE 5.1

RARE-EARTH LASER CHARACTERISTICS

Atomic Number	Ion	Host Material	Wave-length,	Highest oper.	Notes (Typical) (Threshold Values)
60	Nd^{3+}	LaF_3	1.0399	77°K	(75 J)
		LaF_3	1.05*	20°K	
		$PbMoO_4$	1.0586	295°K	(60 J)
		SrF_2	1.0437	77°K	A 1.0370 line at 95°K
		$SrMoO_4$	1.06*	295°K	(17 J and up)
		$SiWO_4$	1.06*	295°K	(5 J at 77°K)
		Y_2O_2	1.073	77°K	(260 J)
		Y_2O_3	1.078	77°K	(600 J)
		Glass	0.9180	80°K	(700 J)
		Glass	1.06	295°K	Pulsed and cw
		Glass	1.37	295°K	(460 J)
62	SM^{2+}	CaI_2	0.7085	4.2°K	
		SrI_2	0.6969	4.2°K	
63	Eu^{3+}	Y_1O_1	0.6113	220°K	(128 J)
64	Gd^{3+}	Glass	0.3125	78°K	(4700 J)
66	Dy^{2+}	CaF_2	2.36	77°K	Pulsed (I J) and cw
67	Ho^{3+}	$Ca(NbO_3)_2$	2.047	77°K	
		CaF_2	2.092	77°K	(260 J)
		$CaWO_4$	2.046	77°K	(80 J)
		$CaWO_4$	2.059	77°K	(250 J)
		Glass	2.046	78°K	(3600 J)
68	Er^{3+}	CaF_2	1.617	77°K	(1000 J)
		$Ca(NbO_3)_2$	1.61	77°K	
		$CaWO_4$	1.612	77°K	(800 J)
69	Tm^{3+}	$Ca(NbO_3)_2$	1.91	77°K	
		$CaWO_4$	1.911	77°K	(60 J)
		SrF_2	1.972	77°K	(1600 J)
69	Tm^{3+}	CaF_2	1.116	27°K	Pulsed and cw
70	Yb^{+3}	Glass	1.015	78°K	(3400 J)
92	U^{+3}	BaF_2	2.556	20°K	(12 J)
		CaF_2	2.24	77°K	
		CaF_2	2.51	295°K	
		CaF_2	2.57	78°K	
		CaF_2	2.613	300°K	(1200 J at 300°K, 2 J at 20°K)
		SrF_2	2.407	90°K	(38 J at 90°K, 8 J at 20°K)

*Approximate wavelength for a cluster of lines.

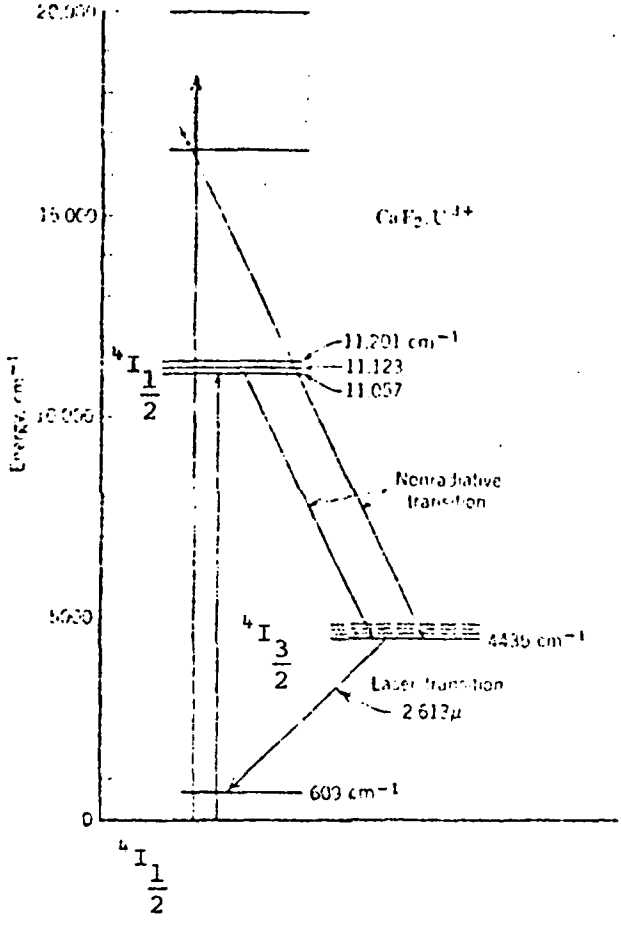

FIGURE 5.1. THE ABSORPTION-FLUORESCENCE CYCLE OF THE 2.613 MICRON TRANSITION IN $CaF_2:U^{3+}$.

are similar in structure although not as uncomplicated, with Nd^{3+} having the widest pumping bands for both collisional and photon absorption. Fluorescence lifetimes are generally around 300μs allowing for the possibility of both pulsed and cw nuclear pumping.

Four major areas of investigation are required with respect to the unknowns of LNPL.

1. Microscopic inhomogeniety of energy deposition.
2. Uranium salt quenching of Nd^{+3} laser states.
3. Radiation damage to lasent.
4. Pumping efficiency

Although the pump energy deposition is homogeneous on a macroscopic scale, there is a quantified inhomogeneity associated with the deposition of each fragment or gamma.

The range of a fission fragment in a liquid is extremely short (the order of 10^{-3}cm). One could operate the nuclear stage as an amplifier stimulated by a conventional cw probe laser of the correct wavelength. While this looks extremely favorable for a nuclear pumped liquid laser, the fact that the range of the fission fragment is so short has the effect that the liquid gets only excited within the short fission fragment track. This provides for the inhomogeneity of excitation. Only experimental research can clarify if this inhomogeneity can be tolerated or is, in fact, even a problem. The effects of gamma or fast neutron deposition should be less.

Although quenching of Nd^{3+} excited states by the addition of U^{3+} ions is not expected, alterations of the optical efficiency of the total chemical system by the addition of the uranium salts can be expected. Radiation damage to the lasent is not expected to be severe since the solvents are highly polar and similar in most respects to H_2O.

The final unknown in the basic knowledge of liquid systems in a nuclear pumped environment involves the kinetics and energy transfer of the system. How does the lasing excited state populate and how efficiently is this accomplished?

Extensions of LNPL technology to high power suggest the onset of several problems: first the removal of heat and then the effects on beam quality due to thermal gradients and fluid flow. Since this system may be pulsed, laser energy can be removed before cascade to thermal upset occurs. In CW operation as a gain cell, beam quality is not as difficult a problem. With the proper tailoring of the flow and design for heat removal, beam transmission quality could be excellent.

For flashlamp pumped Nd^{3+}:$POCl_3$ lasers, efficiency is near 2%. A typical operating solution reactor (Kinglet Reactor at LASL) with 31.4 cm bore and 75.4 cm length has an expected neutron flux of $1 \times 10^{15}/cm^2 sec$. With a 1% efficiency of fission fragment deposition to laser output, this small system would have a laser output of 1.4 mW, CW.

5.6 SUMMARY

A ^3He:Xe nuclear pumped flashlamp laser system based on a burst reactor neutron source has been constructed. The optical output of the flashlamp exceeds 500 joules from 170 nm Xe_2^* fluorescence and 200 joules from Xe^* and the Xe continuum in the visible. The XeF_2 photolysis XeF (C-A) laser system (483 nm) studied did not lase as expected. Gain (~2%/meter) was observed at a lower level than expected. An alternate laser output at 370 nm from S^{III} is suspected. The concept of "parasitic amplification" was developed to explain the discrepancy between calculated gain and lasing and the observed results. Alternate nuclear flashlamp laser concepts and direct nuclear pumped laser systems are reviewed.

REFERENCES

1. Bischel, W.K., D. J. Ekstrom, and D.C. Lorents, "Photolytically Pumped XeF(C-A) Blue-Green Laser," Proceedings of the International Conference on Lasers '79.

2. Bondareu, A.S., et al., "New Low-Toxicity Inorganic Nd^{3+} - Activated Liquid Medium for Lasers," Sov. J. Quant. Electron., Vol. 6, No. 2, pp. 202-204, February, 1976 (APS).

3. Brau, C. A., et al., Excimer Lasers, Topics in Applied Physics, Vol. 30, 1979, 88-99.

4. Cooper, H.G., and P. K. Cheo, "Ion Laser Oscillations in Sulfur," Physics of Quantum Electronics, 690-697, Kelley, Lax, Tannenwald, Ed., McGraw-Hill 1966.

5. DeYoung, R.J., N.W. Jalufka, and F. Hohl, "Direct Nuclear-Pumped Lasers Using the $^3He(n,p)^3T$ Reaction," AIAA 16th Aerospace Sciences Meeting, Huntsville, Ala., Jan. 16-18, 1978.

6. DeYoung, R.J., NPL Workshop, NASA Langley, June 1979.

7. Fisher, Ed, Private Communication, July 1979.

8. Fuller, J., University of Florida, CF_3I NPL exp., unpublished.

9. Goncz, J. H. and P.B. Newell, "Spectra of Pulsed and Continuous Xenon Discharges," Optical Soc. of Am., Vol. 56, No. 1, 87-92, Jan 1966.

10. Hutchinson, M.H.R., "Vacuum Ultraviolet Excimer Lasers," Applied Optics Vol. 19, No. 23, Dec 1980.

11. Jalufka, N.W., NPL Workshop, NASA Langley, June 1979.

12. Kline, L.E., L.J. Denes, P.J. Chanty, "XeF B and C State Kinetics with Self-Sustained Discharge Pumping," Excimer Lasers Technical Digest, Sept. 11, 1979.

13. Lim, S., and E.R. Fisher, Private Communication, June 1979.

14. Lim, S., and E.R. Fisher, "Modeling and Analysis of Nuclear Pumped XeF(C-A) Laser Systems," Final Report USA/BMD DASG60-79-C0056, Feb. 1981.

15. Miley, G.H., et al., "Production of XeF(B) by Nuclear Pumping," Proceedings of the International Conference on Lasers '78.

16. Rowe, M.J., R.H. Liang, and R.T. Schneider, "Nuclear Pumped CO_2 Transfer Laser," IEEE International Conference on Plasma Science, May 1980.

17. Samelson, H and R. Kocher, "High Energy Pulsed Liquid Laser," AD-787895.

18. Walters, R.A., J.D. Cox, and R.T. Schneider, "UV Diagnostics of Charged Particle Excited Gases," Final Technical Report, BMD-ATC DASG60-78-C0045, May 22, 1979.

19. Walters, R.A., J.D. Cox, and R.T. Schneider, "Gain and Lasing in Nuclear Excited Laser Systems," Qrtrly. Rept. BMD-ATC DASG60-74-0083, June 1979.

APPENDIX I

SAFETY ANALYSIS REPORT

21 March 1980

TEST PLAN AND SAFETY ANALYSIS:

NUCLEAR FLASHLAMP LASER EXPERIMENT

(APRD Test #X4-80)

By

R. A. Walters (University of Florida)

and

A. H. Kazi (Army Pulse Radiation Division)

PURPOSE OF REACTOR TEST:

To determine the gain per meter and to observe lasing in XeF^* (C) photolytically pumped by Xe_2^* VUV photon emission at 170.0 nm.

TABLE OF CONTENTS

1.0 INTRODUCTION

Nuclear "Flashlamp" photolytic pumping uncouples the process of nuclear excitation from the laser kinetics. Coupling is obtained only by photon transmission through a barrier.

The research apparatus is pictured in Figure 1. A description of the excitation process occurring during irradiation accompanies the physical description of the research apparatus.

2.0 RESEARCH APPARATUS

2.1 Physical Placement

The laser/gain cell was designed to "surround" the reactor in one plane in order to optimize cavity length. The cell structure is mounted on an aluminum optical mount with appropriate spacing for insertion of the reactor in the center. The supporting gas manifold system is placed in an adjacent position, approximately 8m from the reactor. Optical diagnostics systems will be placed in a remote shielded location. For the gain study, a 1 watt argon ion laser will be placed on the reactor cell floor approximately 75m from the experiment.

2.2 Flux Trap

The mode of excitation of the Xe_2^* flashlamp is via energy deposition of the 750 KeV fission products of thermal neutron fissioned ^3He. The thermal neutron pulse will be produced in a polyethelene flux trap 15 cm (6 inches) in diameter and about 50 cm long. Four such flux traps will be placed adjacent to and around the reactor. The flux traps are covered with a 0.125 inch thick decoupling material containing about 50 w/o $^{10}B_4C$. This is similar to the decoupling material on the reactor. Experience with many pulse operations performed at APRD on flux traps for NASA has shown this to be satisfactory for decoupling the polyethylene in the flux traps from the reactor core.

2.3 Flashlamp

The flashlamp is of coaxial design. The outer cylinder is 33 mm OD quartz with a 1.5 mm wall. Its pressure capability is to 80 psi with a safety factor of 10. The inner cylinder is 9 mm OD, 1 MM wall, Suprasil (Quartz with a special polish). Its pressure capabilities exceed the outer cylinder because all stresses will be compressive. The volume (289.4 cm^3) between the tubes will be filled with 3.2 atmospheres ^3He and 1 atm Xe. Upon exposure to thermal neutrons, the ^3He will fission ($^3He(n,p)T$). The reaction products will excite the 170 mm band of Xe_2^*

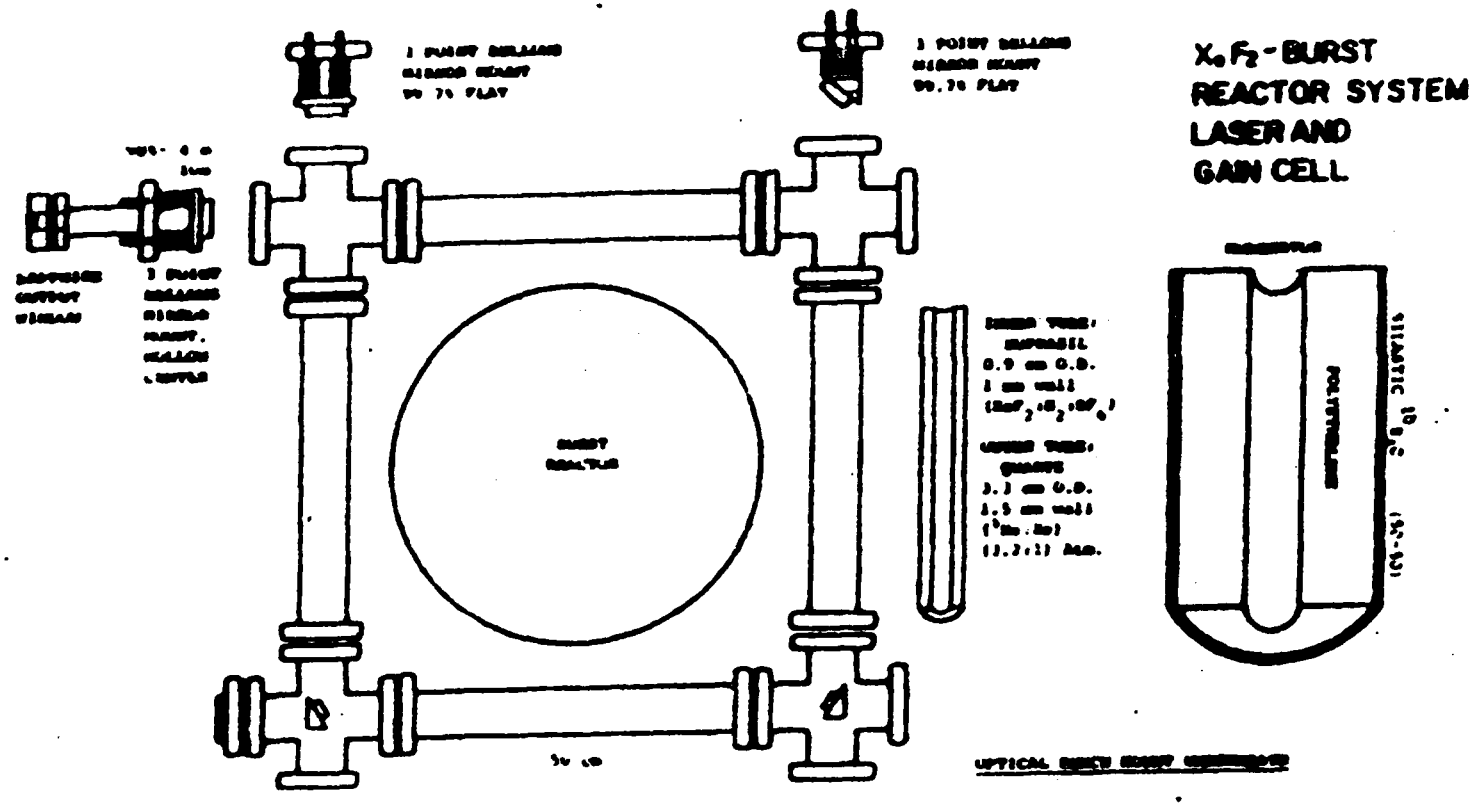

Figure 1.

with a 67% emission efficiency. The 170 nm photons will pass through the suprasil inner wall and be absorbed by XeF_2 in the center of the coaxial section (which is open). The flashlamps are prefilled at the University of Florida and will remain sealed at the reactor facility. Final design parameters of the nuclear flashlamp apparatus are listed in Table I.

TABLE I. FINAL DESIGN PARAMETERS OF NUCLEAR FLASHLAMP APPARATUS

1.	Size of Laser Ring	54.6 cm
2.	Center of Tube to Reactor Centerline	27.3 cm
3.	Reactor Centerline to Edge of Flux Trap	19.15 cm
4.	Diameter of Space Allowed for Reactor	38.3 cm (15.08 inches)
5.	Flashlamp Length	45 cm
6.	Volume	289.4 cm^2 x 4 = 1.16 liters

The coaxial quartz system is designed with heavy endcaps of transition glass, properly annealed. The stresses on the inner tube are compressive. The outer tube has a pressure specification of 80 psia with a safety factor of 10. With a careful check for small scratches etc., one can in the absence of any deformation place the capability of the tube to 400 psia with a safety factor of 2.

2.4 Optical System and Outer Chamber

A flashlamp assembly is placed into stainless steel 1 1/2" OD tubes in each leg of the laser. Optical mounts that are fluorine compatible and vacuum sealed are placed in 5 positions as noted in Figure 1. All fittings are standard Varian, based on the 952-5050 (2-3/4") cross. Copper gaskets are used. Three viewing ports (954-5127) are located at the cross corners. These aid in alignment. The output port is a sapphire window (954-5140). During the experimental run, the total inner chamber will be filled with N_2 at 2 atmospheres. XeF_2, 4 to 10 torr, and SF_6 at 2 torr. This mixture is depleted (XeF_2) after each run and must be replaced. During the pulse, the 170 nm photons are absorbed by XeF_2. XeF_2 dissociates producing XeF^* which relaxes to the C state. The C-A transitions are then lased at 488 nm. The inversion is 100%.

The optical system contains 5 mirrors, 4 of which are 99.7% reflective at 488 nm and the fifth, the output mirror 98% reflective.

2.5 Gas Manifold

The gas manifold or fill and empty system contains appropriate valves, regulators, and pump systems to service the gas needs of the experiment. This system is self-contained with only a large N_2 bottle and vacuum roughing pump external to the structure. The vacuum pump exits into a cleanup system that will be composed of two containers. 1) empty, 2) water. If any tritium is released it will be captured by this system.

2.6 Optical Diagnostic Equipment

Laser:

1. HeNe alignment laser (removed before burst)
2. Beam Splitter
3. 1 Fiber Optic Cable
4. Optical Multichannel Analyser (OMA)
5. Optical Diode
6. Oscilloscope - camera.
7. FM Tape Recorder - 4 channels.

The OMA will observe the spectral output of the laser and the diode will record on the scope camera and FM recorder the time dependent output of the laser.

Gain:

1. Output Mirror Removed
2. Ar^+ Laser in Reactor Cell
3. Beam Splitter
4. 2 Fiber Optic Cables
5. 2 Optical Diodes
6. Differential Oscilloscope - camera
7. FM Tape recorder

The two diodes will measure differential gain between a prime Ar^+ beam at 488 nm and one that traverses the cavity.

3.0 ENERGY RELEASE IN FLASHLAMP

3.1 Thermal Flux

Based on thermal flux measurements made on a NASA flux trap, the estimated average thermal flux is 5.8×10^{16} n/cm^2-s at a pulse yield of 1×10^{17} fissions. With an effective thermal pulse width of 2×10^{-4} s, the average thermal fluence is 1.2×10^{13} n/cm^2. The thermal flux will be measured using gold foils in a low power steady state run, or with a Cobalt-59 self powered detector, prior to tests at full pulse yield.

3.2 Helium-3 Inventory

The number of ^3He atoms at STP in all four tubes is

$$n = \frac{N \cdot A}{m} = \frac{.177g}{\ell\text{-atm}} \times \frac{3.2 \text{ atm} \times 1\text{-}16\ \ell}{3g/\text{mole}}$$

$$\times \quad 6.023 \times 10^{23} \text{ atoms/mole}$$

$$= \quad 1.32 \times 10^{23} \text{ atoms}$$

which corresponds to 3.3×10^{22} atoms/tube. This number is conservative since it is not corrected for room temperature.

3.3 Energy Release and Pressure Rise

The energy release per ^3He (n,p) ^3H reaction is 0.76 MeV = 1.22×10^{-13} joules, and the thermal neutron cross section is 5.3×10^{-21} cm^2. The energy release per 1×10^{17} fissions pulse per tube is therefore 1.22×10^{-13} joules x 5.3×10^{-21} cm^2 x 1.2×10^{13} n/cm^2 x 3.3×10^{22} atoms = 255 joules. The corresponding temperature rise is 163 ^oK.

This energy release corresponds to a pressure increase of 2.3 atm. The static pressure is 4.2 atm so that the maximum pressure is 6.5 atm or 96.1 psia. This exceeds the 80 psia specification. Note however that the above pressure rise calculation is conservative since at least 50% of the energy released will be transferred to the 170nm VUV Band. Part of this will go through the walls and into the center region. The shock wave produced by this heating will also probably be minor since ΔT is moderate. The complex shape of the container and the uniform excitation of the volume tend to discount focussing of a shock wave on a particular structure.

If one of the tubes were to break, the stainless steel outer structure and its extensive expansion capability will contain all refuse. An unexplained change in the outer chamber pressure will indicate that one of the tubes has ruptured.

4.0 TRITIUM PRODUCTION

The total number of tritium atoms produced per pulse is

$$1.32 \times 10^{23} \text{ atoms} \times 5.3 \times 10^{-21} \text{ cm}^2 \times 1.2 \times 10^{13} \text{ n/cm}^2 = 8.3 \times 10^{15}$$

which corresponds to 404 microcuries per pulse in all four tubes. The volume of the reactor silo is about 1.8×10^{10} cm^3 so that the concentration is 2.24×10^{-8} $\mu c/cm^3$. In one week there are typically no more than 16 pulses so that total tritium inventory would be 6.46×10^3 μc and the

concentration, if this were all released, would be 3.6×10^{-7} $\mu c/cm^3$. The MPC (Maximum Permissible Conentration) as given in Part 20, Code of Federal Regulations, dated 1 September 1978, is 5×10^{-6} $\mu c/cm^3$ for restricted areas and 2×10^{-7} $\mu c/cm^3$ for unrestricted areas. The reactor silo is a restricted area. It is therefore evident that the above postulated release of tritium, which is a conservative worst case, would pose no particular problems and is within the realm of routine reactor operation. Nevertheless, a tritium cleanup system is attached to the effluent of the vacuum pump. This cleanup system consists of an empty container to provide overflow security for the exit line and a container of H_2O, through which the effluent will be passed. There is a great possibility that all effluent tritium (if any) will be trapped in the vacuum pump oil.

5.0 REACTIVITY WORTH

From an operational and safety point of view the reactivity worth of an experiment should be kept below about $2.30. The exact reactivity worth of the present experiment can only be determined from a measurement since it depends on the exact material configuration and composition. However, based on reactivity data available on two cylindrical flux traps operated for NASA, the estimated worth is somewhat below $2. This is therefore acceptable. It should be noted that reactivity worth is not really an operational problem since the reactor can always be raised away from the experiment an appropriate distance to obtain the desired reactivity worth.

6.0 OVERALL TEST PLAN

The test plan consists of the following steps to be accomplished in sequence:

1. Check out of apparatus at University of Florida including static pressure test.

2. Set up and alignment of apparatus at APRD. Use will be made of an existing aluminum table 4' x 4', 60.5 inches high, which has a 15 inch diameter hole in the middle.

3. Reactivity calibration, measurement of worth of regulating rod inch, and minipulse to determine pulse rod worth. If the reactivity worth is unacceptable the reactor will be raised slightly.

4. Measurement of thermal flux using gold and cadmium covered gold foils at an exposure of a few hundredwattminutes. The NASA Cobalt-59 self powered flux detector will be installed if available.

5. Pulse operation will commence at a yield of $\sim 3 \times 10^{16}$ fissions and if reactor behavior is satisfactory proceed to 6×10^{16} fissions and to 1×10^{17} fissions. Maximum target yield is 1.1×10^{17} fissions.

6. As noted earlier, during pulse operation, the total inner chamber will be filled with N_2 at 2 atmospheres, XeF_2 at 4 to 10 torr, and SF_6 at 2 torr. This mixture is depleted in XeF_2 after each run and must be replaced. Use is therefore made of the gas handling system after each run.